MECHANOTRANSDUCTION-DEPENDENT CHANGES IN THE CONTRIBUTIONS OF ACTIN ISOFORMS TO THE AUDITORY STEREOCILIA CYTOSKELETON

Exploratory Mode

SARA LEGNY MACIAS PALACIO

Undergraduate thesis for the degree of Biomedical Engineering

A. Catalina Vélez Ortega, Ph.D.

UNIVERSIDAD EIA®
Ser, Saber y Servir
Con Acreditación Institucional

UNIVERSIDAD EIA
BIOMEDICAL ENGINEERING
ENVIGADO
2021

Dedicated to my grandpa, my inspiration, the man who taught me the wonder of science and the value of hard work. Also dedicated to my mom, my role model and constant source of support and encouragement.

ACKNOWLEDGMENTS

Throughout the development of this dissertation I received a great amount of support and assistance.

First, I would like to express my deepest appreciation and gratitude to my advisor Dr. A. Catalina Velez Ortega, your guidance was essential for accomplishing this dissertation. Your help and patience were invaluable to the success of this project; every meeting, comment and question always inspired me to go the extra mile. Thanks for believing in me and my abilities. I am so grateful for your friendly advice in any topic and all the time you dedicated to this thesis despite your busy schedule. I could not have asked for a better mentor.

Special thanks to Claire I. Haston, for your training, endless help and friendship through this process.

I am extremely grateful to my family, especially my mom Eliana and my grandparents Carmen and Rey, without your unconditional support I would not have made it through these five years of college and these months of intense work. Thanks for always being there for me, for your love and your faith in me.

Thanks should also go to my friends, those who have always been there and those who recently came to my life, for supporting me and encouraging me (even in the distance), but also for the fun and all the good times.

Finally, thanks to all the people that somehow enabled this research to be possible.

Supported by NIDCD R21DC017247 to A.C.V.

CONTENTS

page.

LIST OF FIGURES

pg.

LIST OF ANNEXES

RESUMEN

Los estereocilios, proyecciones mecano-sensoriales presentes en la parte superior de las células ciliadas del oído interno, están hechos de filamentos de ambas isoformas citoplasmáticas de actina: β y γ (Furness et al., 2005; Perrin et al., 2010). La ausencia de cualquiera de las dos isoformas mencionadas resulta en el crecimiento normal de los estereocilios pero eventualmente se degeneran (Belyantseva et al., 2009; Perrin et al., 2010). Por otra parte, una disminución en el ingreso basal de Ca^{2+} a través de los canales de transducción mecano-eléctrica (MET) quebranta la estabilidad del citoesqueleto de los estereocilios, llevando a un adelgazamiento y retracción en su estructura (Vélez-Ortega et al., 2017). La actina β tiene una cinética de polimerización y despolimerización más rápida que la actina γ cuando están unidas al Ca^{2+} (Bergeron et al., 2010) así que los cambios en la entrada de Ca^{2+} a las células ciliadas a través de los canales MET, puede afectar a ambas isoformas de maneras diferentes. Es así como se evaluó la existencia de cambios dependientes de la mecanotransducción en la distribución de actina β y γ a lo largo de los estereocilios de las células ciliadas del oído interno.

Explantes del órgano de Corti de ratones tipo silvestre fueron aislados a edades posnatales tempranas y cultivados en condiciones de control o en la presencia de tubocurarina (60 µM), un agente que bloquea los canales MET. Los explantes se fijaron en el momento de ser aislados (frescos) o en puntos de tiempo específicos después de bloquear los canales MET. Dependiendo de la etapa del proyecto, las muestras se procesaron para ser visualizadas con microscopia confocal (por medio de la inmunotinción con anticuerpos marcados con fluoróforos contra las isoformas de actina β y γ) o microscopia electrónica de barrido. Las imágenes obtenidas con microscopia confocal fueron procesadas y medidas utilizando el algoritmo que fue creado.

Se encontró que las proporciones de actina γ/ actina β a lo largo de la longitud de los estereocilios no se vieron afectadas en condiciones de cultivo durante las 48 horas evaluadas. Se presenta evidencia del adelgazamiento y acortamiento en la segunda y tercera fila de estereocilios después de la incubación con tubocurarina. Sin embargo, según la información mostrada acerca de la cuantificación de la fluorescencia, no se encontraron cambios en las proporciones de actina β y γ durante los reordenamientos del citoesqueleto que dependen de la mecanotransducción.

Por lo tanto, se puede afirmar que las diferencias dependientes del Ca^{2+} en las tasas de polimerización y despolimerización entre ambas isoformas de actina, no son el mecanismo principal detrás de los reordenamientos del citoesqueleto de los estereocilios cuando suceden cambios en las concentraciones de Ca^{2+} dentro de las células ciliadas auditivas del oído interno en los mamíferos, considerando que las proporciones de ambas isoformas se mantuvieron en el citoesqueleto de los estereocilios durante este proceso.

Palabras clave: células ciliadas del oído interno, estereocilios, isoformas de actina, canales de mecanotransducción.

ABSTRACT

Stereocilia, mechanosensitive projections on top of the inner ear hair cells, are made of filaments from both cytoplasmatic actin isoforms: β and γ- (Furness et al., 2005; Perrin et al., 2010). The absence of either of these isoforms results in the normal growth of stereocilia but they eventually degenerate (Belyantseva et al., 2009; Perrin et al., 2010). Moreover, a decrease in the resting influx of Ca^{2+} through the mechanotransduction (MET) channels, disrupts the stability of the stereocilia cytoskeleton, leading to thinning and shrinking of stereocilia (Vélez-Ortega et al., 2017). When bound to Ca^{2+}, β- actin has faster polymerization and depolymerization kinetics than γ- actin (Bergeron et al., 2010) so changes in Ca^{2+} influx to the hair cell through MET channels might affect both isoforms in a different way. Therefore, the existence of MET-dependent changes in the distribution of β- and γ- actin along stereocilia lengths in mouse auditory hair cells was evaluated.

Organ of Corti explants from wildtype mice were isolated at early postnatal days and cultured in control conditions or in the presence of the MET channel blocker tubocurarine (60 µM). Explants were fixed when freshly isolated or at specific time points after MET channel blockage. Depending on the stage of the project, samples were either immunostained with fluorescently-labeled antibodies against β- and γ-actin isoforms and imaged via confocal microscopy, or prepared for scanning electron microscopy (SEM) imaging. Obtained images from confocal microscopy were processed and measured using the created algorithm.

It was found that the ratios of γ- to β- actin along the length of stereocilia were not affected in culture conditions up to 48 hours. Evidence was provided on the thinning and shortening of second and third row of stereocilia after the incubation with tubocurarine. Nevertheless, according to the presented data on the fluorescence quantification, no changes in the ratio of β- and γ- actin were found during these MET-dependent cytoskeleton rearrangements.

Therefore, it can be affirmed that Ca^{2+}-dependent differences in polymerization and depolymerization rates between β- and γ- actin are not the main mechanism driving stereocilia cytoskeleton rearrangements upon changes in intracellular Ca^{2+} concentrations in mammalian auditory hair cells, since the proportions of both actin isoforms were maintained in the stereocilia cytoskeleton during this process.

Keywords: hair cells, stereocilia, actin isoforms, mechanotransduction channels.

INTRODUCTION

Stereocilia are specialized microvilli that are present on top of the inner ear hair cells, organized in a staircase shape, meaning that their heights increase when advancing through the bundle (reviewed in (Furness & Hackney, 2006)). These structures are made of actin, specifically a core constituted by a paracrystal array of parallel filaments containing both β- and γ- actin (Furness et al., 2005; Perrin et al., 2010;Tilney et al., 1980). When the genes associated with these isoforms are mutated in humans, this leads to syndromic and non-syndromic hearing loss.

The major function of the stereocilia bundles is converting the mechanical stimuli of sound waves in electrochemical signals that can be transmitted to the brain (reviewed by (Orr et al., 2006)). This process is called mechanotransduction (MET) and is possible through the MET channels which are located at tips of stereocilia in the shorter rows (Beurg et al., 2009).

When activity in these channels is decreased, the Ca^{2+} influx to the cell is altered, which has an effect on stereocilia cytoskeleton morphology (Vélez-Ortega et al., 2017). Furthermore, it was demonstrated that β- and γ- actin have different polymerization and depolymerization kinetics in the presence of calcium (Bergeron et al., 2010).

With the presented information in mind, this project evaluated if there is a change on how actin isoforms are distributed along the length of stereocilia when calcium concentrations inside the cell are altered. All experiments were performed in the laboratory of Dr. A. Catalina Vélez-Ortega in the Department of Physiology at the University of Kentucky in Lexington, Kentucky, USA.

Theoretical valuable information is provided below for the understanding of the terms used in the course of this project while referring to structures, techniques and processes. In addition, there is a section explaining in detail all the methods employed for the development of the experiments and the subsequent data analysis.

Next, the results of the project are presented in a logical way to determine if there is a change on the actin isoforms distribution, along with a bibliographic review that allows an insight of the reasons behind these findings through the comparison with outcomes from other authors or the similarities or differences between studies.

Finally, conclusions and some future directions for further understanding on the related phenomena are presented.

1. PRELIMINARY

1.1 RESEARCH PROBLEM

Hearing is a complex sense that results from mechanical stimuli being converted into electrochemical signals and then transmitted to the brain (reviewed by (Orr et al., 2006)). This process is known as mechanotransduction (MET), alternatively stated by Pepermans & Petit (2015), as “the conversion of the sound-evoked mechanical stimulus into a membrane receptor potential”. The structures that make it possible are the MET channels, which are non-selective cation channels mechanically gated by small extracellular structures known as tip links (Assad et al., 1991; Corey & Hudspeth, 1979; Pickles et al., 1984).

Tip links are protein made thin filaments that connect each stereocilium with another in an adjacent taller row and, whenever the stereocilia bundle deflects towards the tallest row, tip links enable the gating of the MET channels at the tips of the transducing stereocilia as shown in figure 1. At their resting position, tip links are sufficiently tensioned to assure MET reactions to even the tiniest bundle deflections (Corey & Hudspeth, 1979).

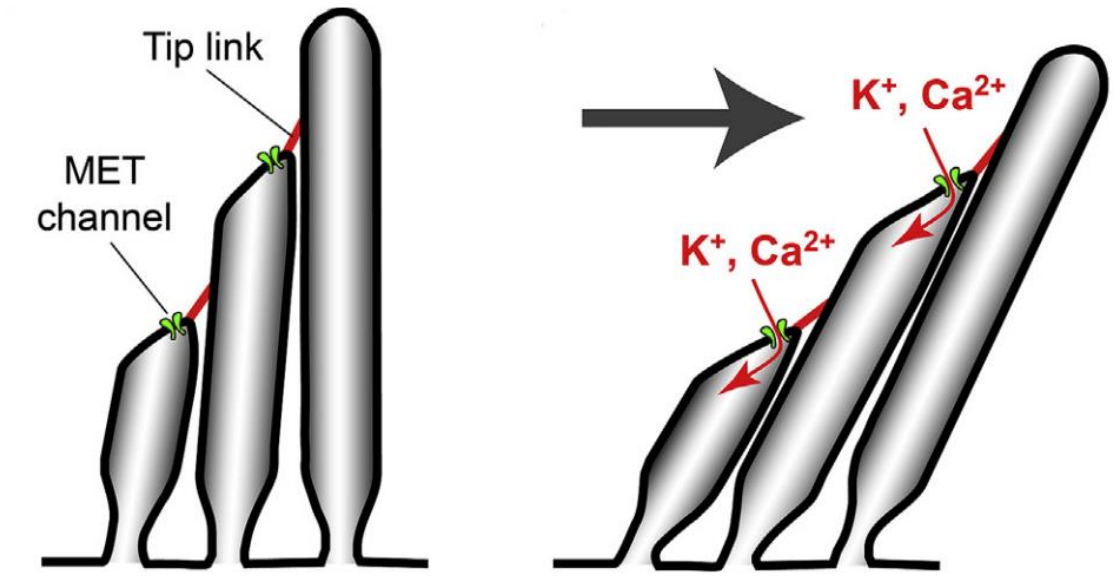

Figure 1: Drawing illustrating stereocilia morphology before and during sound exposure (where sound, represented by the arrow, deflects the bundle allowing the opening of the MET channels).(Vélez-Ortega & Frolenkov, 2019).

To comprehend the aforementioned, it has been demonstrated that deflections as small as 1-100 nm of the stereocilia bundles, can be transmitted via tip links and lead to the opening of the MET channels (reviewed by (Fettiplace & Kim, 2014)). Moreover, it has been estimated that the mammalian hair cells can detect sound-induced vibrations as small as 1 Ångstrom (0.1 nm) (Robles & Ruggero, 2001). This tension of the tip links at rest, leads to the opening of a subset of MET channels and thus to the constant entry of calcium into the hair cells even in resting conditions.

On the other hand, stereocilia are rigid microvilli with various lengths (reviewed by (Pepermans & Petit, 2015)) in a staircase-like morphology (Tilney et al., 1980). The core of these structures is constituted by a paracrystal array of parallel actin filaments (Tilney et al., 1980). It is known that hair cells express both β- and γ-actin but there are discrepancies between authors and species on their distribution (reviewed in (Vélez-Ortega & Frolenkov, 2019)).

Despite that, it's been demonstrated that the transducing stereocilia have conformational changes with certain stimuli, in particular, they get shorter after the blockage of the MET channels with pharmacological drugs or the disruption of the tip links, but stereocilia regrow after removing the blockage or after the tip links regenerate (Vélez-Ortega et al., 2017). This activity-dependent remodeling of the stereocilia cytoskeleton was shown to depend on changes in the influx of calcium through MET channels that are partially open at rest (Vélez-Ortega et al., 2017). During this process there might be some changes in the percentage of actin isoforms, considering that β- and γ-actin exhibit different polymerization and depolymerization rates depending on calcium concentrations (Bergeron et al., 2010) and that some authors claim different functions for each isoform, for example, Belyantseva et al. (2009), hypothesized that γ-actin could repair the stereocilia after *in-vivo* damage by showing that γ-actin fills noise-induced gaps in the stereocilia cores.

In order to make an effort to comprehend how the MET-dependent changes to the stereocilia cytoskeleton are accomplished, it's crucial to answer: how do the actin isoforms change their proportions after a decrease in MET channel activity?

1.2 PROJECT OBJECTIVES

1.2.1 General Objective

To identify the relative contribution of β- vs. γ- actin isoforms during the stereocilia remodeling after a decrease in mechanotransduction (MET) channel activity.

1.2.2 Specific Objectives

- To create an algorithm for the quantification of β- and γ- actin along the stereocilia length.
- To compare whether the cell culture of the inner ear tissue affects the ratio of β- and γ- actin in stereocilia.
- To evaluate the ratio of β- and γ- actin in stereocilia at two time points after the blockage of the MET channels.

1.3 STATE OF ART

1.3.1 Previous Work

Many efforts have been done to achieve the understanding of human body and inner ear is not the exception. Some publications that are relevant for the significance and development of this project are:

- Furness et al. (2005), showed that both β- and γ- actin are present in the stereocilia cytoskeleton, but most important, they stablished their specific distribution (γ-actin all over the stereocilia and β-actin concentrated at the periphery of stereocilia in a ring-shaped crossed section). These studies were done in cochleae extracted from adult guinea pigs.

- Belyantseva et al. (2009), generated mice lacking γ-actin expression and concluded that γ-actin is not necessary to build stereocilia but is responsible for the maintenance of the actin cytoskeleton. In fact, they also demonstrated its repairing role by showing the appearance of γ-actin filled gaps in stereocilia cores after *in-vivo* damage of mouse hair bundles. Supporting this statement, Perrin et al. (2010) used knock-out mice to show that neither β- or γ- actin is essential for stereocilia or hearing development but aging mice exhibited stereocilia degeneration and progressive hearing loss. It shows how both maintenance pathways are important for keeping auditory function despite β- and γ- actin colocalization.

- Kawashima et al. (2011), identified TMC1 and TMC2 as potential proteins that make up MET channels. Later, Pan et al. (2018) established that TMC1 forms the pore of MET channels in hair cells from vertebrates.

Nevertheless, the most important antecedents for this project are those related to stereocilia stability changes associated with the MET current, specifically how Ca^{2+} influx through MET channels may have a variable effect on actin isoforms. These are:

- Bergeron et al. (2010), found that γ-actin exhibits slower polymerization and depolymerization kinetics than β-actin, when bound to Ca^{2+}. As a consequence, important differences might be found in the actin-rich cochlear hair bundles, where mM calcium concentrations exist.

- Caberlotto et al. (2011a) and Caberlotto et al. (2011b) used mutant mice that had impaired MET activity and hinted that mechanotransduction was important for the proper actin polymerization within stereocilia.

- Vélez-Ortega et al. (2017), stated that Ca^{2+} influx through the resting MET current is essential for the stability of stereocilia. When there is a resting current in MET

channels, actin remodeling may be limited to the tips of stereocilia but, when they blocked or disrupted MET channel activity, transducing stereocilia retracted. This was the first experimental evidence showing that stereocilia morphology can be controlled by the MET current.

- Krey et al. (2020), found out that MET channel activity keeps the identity and height of each stereocilia row as well as controlling how new actin filaments are added to grow stereocilia diameter by studying stereocilia development in mice that had mutations impairing MET channel activity.

1.3.2 Theoretical Framework

1.3.2.1 Hearing Overview

As explained in detail in Widmaier et al. (2019) , hearing is a mechanical sense where sound waves travel across the involved structures to finally be transmitted to the brain. This process goes through three regions: outer, middle and inner ear (Figure 2).

The first step occurs in the outer ear when the sound waves enter the auditory canal and travel through it, the shapes of the structures in this region contribute to amplify and direct the waves until they reach the tympanic membrane and make it vibrate at the same frequency as the waves.

This vibration is transmitted and amplified in the middle ear; a cavity filled with air that is located in the temporal bone of the skull. This amplification is done by the ossicles (malleus, incus and stapes), three small bones that transfer the vibrations to the oval window, a membrane that separates the middle and the inner ear.

Then, the produced pressure goes through the cochlea, a spiral-shaped space filled with liquid. Inside the cochlea sits the organ of Corti which contains the hair cells, mechanoreceptors that convert the received pressure-induced vibrations into action potentials in the afferent neurons that eventually reach the brain to be interpreted as speech, music, or other environmental sounds.

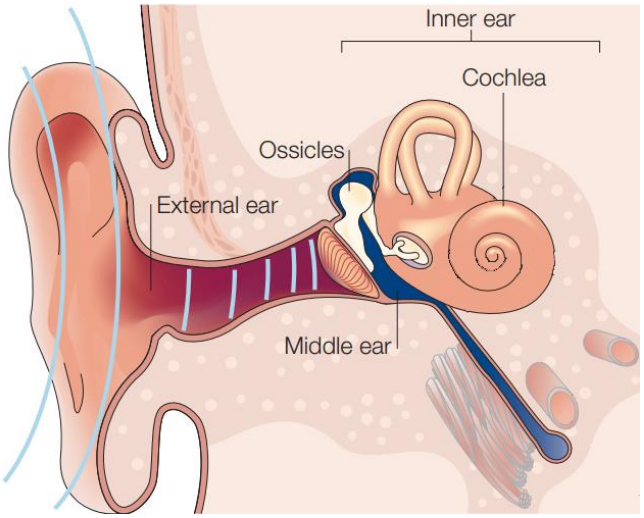

Figure 2: Representation from outer, middle and inner ear. Modified from (Frolenkov et al., 2004)

Even if all the different sounds follow the same route to the inner ear, here they are processed in different regions. This is due to the basilar membrane which has varying degrees of stiffness across its length, this property allows different frequencies to resonate in different regions of the organ of Corti as shown in figure 3. Low frequency sounds stimulate the apex, medium-frequency waves affect the middle and high frequency sounds stimulate the base (Encyclopedia Britannica, n.d.).

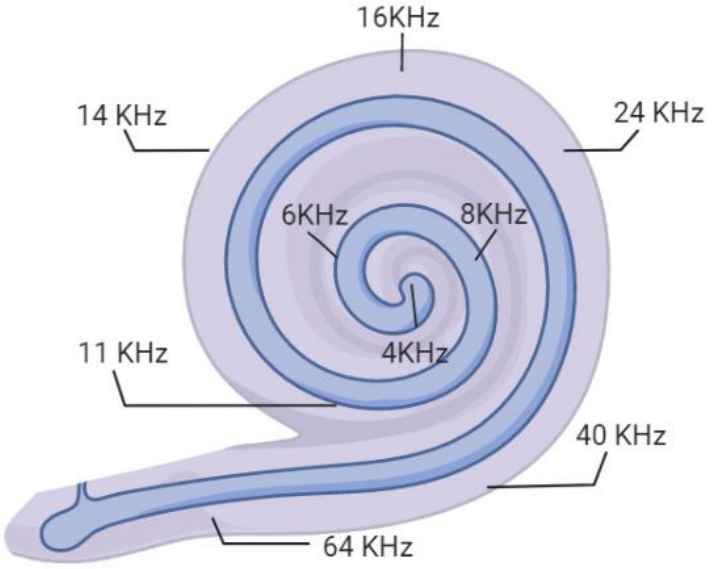

Figure 3: Frequency map through the organ of Corti in mice. Image created in Biorender.

1.3.2.2 Hearing loss

Congenital deafness, defined as hearing loss that occurs at birth, is one of the most common chronic illnesses in children according to Korver et al. (2017). Based on information gathered by the Centers for Disease Control and Prevention (CDC), “The prevalence of hearing loss in 2017 was 1.7 per 1,000 babies screened for hearing loss” in the United States (CDC, 2020).

Hearing loss can be caused by a variety of factors such as cortical malformation, intracranial hemorrhage, internal ear malformations, auditory neuropathy (Faistauer et al., 2021), ototoxic medicines (Dillard et al., 2021), exposure to loud sounds (NIH, 2019), congenital infections like Congenital Cytomegalovirus (CMV) infection (Riga et al., 2018), hypoxia, hyperbilirubinemia (Roizen, 2003), genetic factors (Avettand-Fenoël et al., 2013), among others.

Particularly, genetic factors are thought to be responsible for around half of all congenital hearing loss cases (Ding et al., 2021) and these mutations can affect any component of the auditory system, including inner ear homeostasis and mechanotransduction (MET) (Korver

et al., 2017). Similarly, noise-induced hearing loss was reported to affect about 1 in 4 adults in the United States (NIH, 2019).

1.3.2.3 Hair cells

The cochlear epithelium consists of sensory cells, called hair cells, and several other types of supporting cells and other extracellular elements like the tectorial membrane and the basilar membrane, as shown in figure 4. Besides, hair cells are innervated with both afferent and efferent paths (Reviewed by (Raphael & Altschuler, 2003)). These sensory cells are usually a small percentage of all the cells in the cochlea, this is especially important to consider when talking about keeping hearing capacity during the lifespan of an organism since in mammals, there is no regeneration of the hair cells. Whenever tissue damage occurs, support cells make permanent scars by filling the gap and even if the epithelium is repaired, the replacement is done with unspecialized cells (Oesterle, 2013; Raphael et al., 2007)

The hair cells, located on the organ of Corti, are on the edge between two regions that contain two different solutions: the endolymph and the perilymph. The projections on top of the cells (stereocilia) are in contact with endolymph, an unusual extracellular fluid with high concentration of K^+, meanwhile the rest of the cell (*i.e.* the basolateral membrane) is in contact with the perilymph, a solution rich in Na^+ and low in K^+, similar to the cerebrospinal fluid (Salt & Hirose, 2018).

These cells are organized in rows according to their type. There are three rows of outer hair cells and one row of inner hair cells as shown in figure 4.

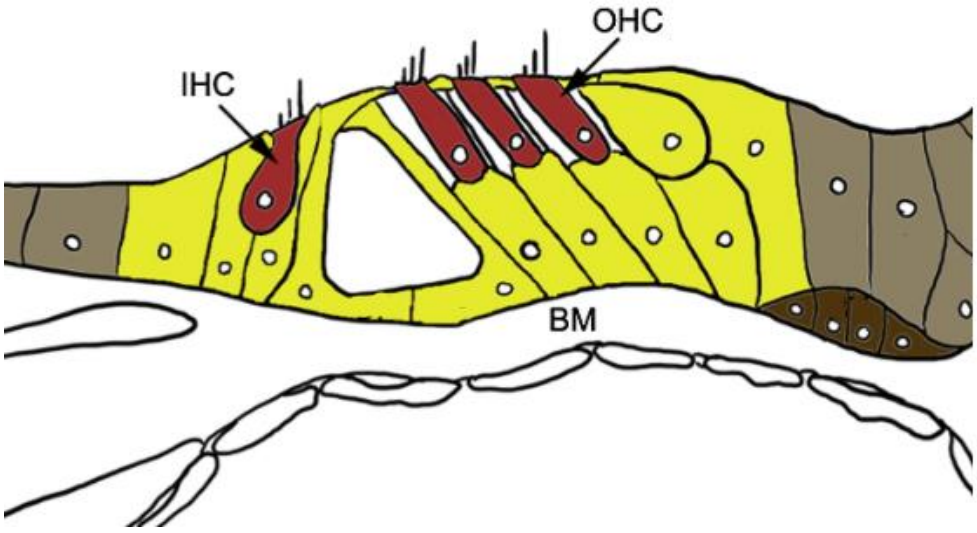

Figure 4: Diagram of cochlear epithelium in mammalians. Sensory cells -inner hair cells (IHC) and outer hair cells (OHC)- in red and supporting cells in yellow. The basilar membrane is also illustrated (BM). Modified from (Oesterle, 2013).

Hair cells differ in their innervation pattern since 20 outer hair cells are innervated by one afferent neuron, but one inner hair cell is innervated by 20 afferent neurons, likewise, it's feasible to state that there is a physiological discrepancy between them and this is confirmed knowing that inner hair cells are crucial for direct afferent transmission of sound to the brain meanwhile outer hair cells play a modulatory role as they are in charge of amplifying the sounds that enter the cochlea (Qing & Mao-li, 2009).

1.3.2.4 Stereocilia - Hair cell bundle

On top of the sensory cells, there is a stereocilia bundle, a group of specialized microvilli organized in a staircase-shape with increasing heights across the bundle (reviewed in (Furness & Hackney, 2006)). These structures allow to detect mechanical stimuli and convert it to electrical signs through their transduction machinery (For a review on the mechanotransduction machinery in inner ear hair cells see (Fettiplace & Kim, 2014)).

This bundle of mammalian auditory hair cells contains three rows of individual stereocilia and one kinocilium, a cilium located at the back of the bundle (reviewed in (Frolenkov et al., 2004)). In the mammalian cochlea, stereocilia bundles are arranged in a v shape in outer hair cells and a wide-open c shape in inner hair cells as it can be seen in figure 5.

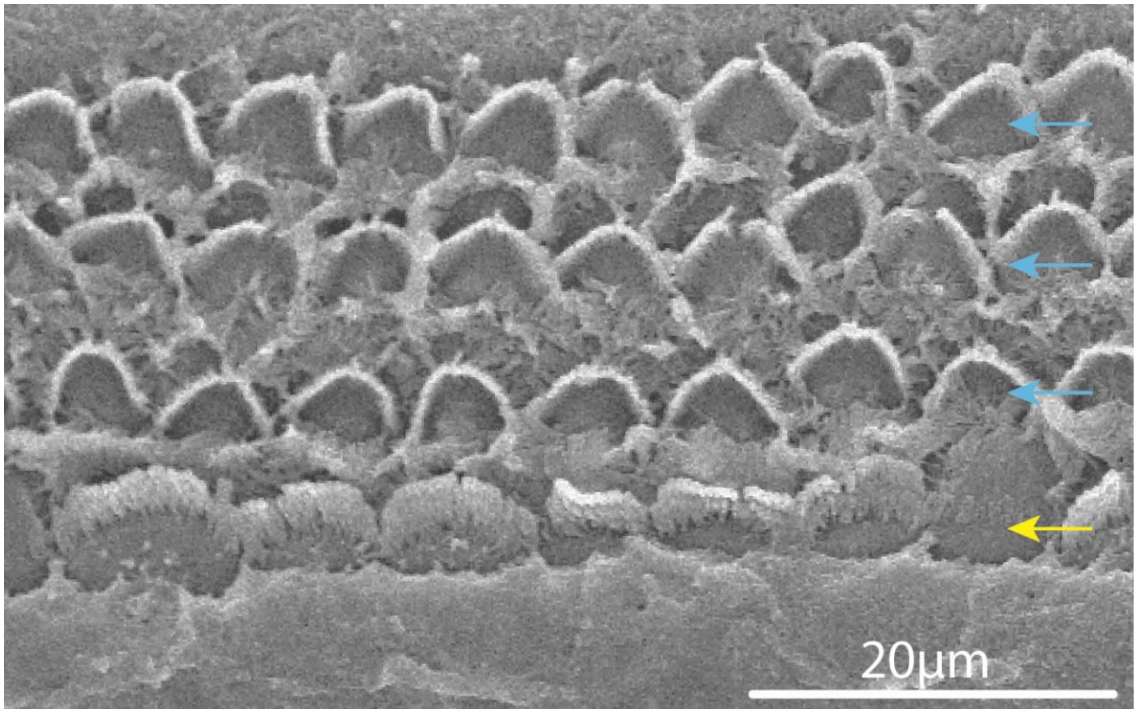

Figure 5: SEM image of the middle region from the organ or Corti. Arrows point to the row of inner hair cells (yellow) and the three rows of outer hair cells (blue).

Mammalian hair cells usually have 3 rows of stereocilia while non mammalian bundles usually have more rows (Reviewed in (Ó Maoiléidigh & Ricci, 2019)).

Stereocilia are usually very uniform along their length except at the bottom where they have a taper in the junction with the cell body. This decrease in thickness is explained by the termination of most actin fibers in this region, which implies that only the actin filaments from the center of the stereocilia reach the body of the cells (reviewed in (Frolenkov et al., 2004)).

At the base of each stereocilium there is a structure called rootlet, a dense core of firmly packed actin fibers that goes down to the cuticular plate and anchors the stereocilium to this actin meshwork (Pacentine et al., 2020).

The cytoskeleton of the stereocilia is also made of actin, specifically polarized parallel filaments that are organized into a rigid structure (DeRosier et al., 1980; Tilney et al., 1980). Each mouse stereocilium contains around 400.000 actin monomers (Krey et al., 2016) distributed between both β- and γ- actin.

1.3.2.5 Actin

Actin is a cytoskeletal protein that can be found in every cell of the body since its fundamental for many roles like structural support, migration, cell division, among others (Suresh & Diaz, 2021). The reason behind the presence of this protein in so many functions is that actin is composed of different isoforms. Mammals and birds have six different genes and each one encodes an isoform but all of them are similar to each other, sharing no less than 93% of their sequences (reviewed by (Perrin & Ervasti, 2010)). The way in which these isoforms are distributed seems to be tissue specific, there are four muscle isoforms (α skeletal-actin, α cardiac-actin, α smooth-actin, and γ smooth-actin) and two non-muscle (β cytoplasmic-actin and γ cytoplasmic-actin) isoforms (Drummond et al., 2012).

The cytoplasmic isoforms are almost equal, they just differ on their N-termini by four amino acids (reviewed in (Perrin & Ervasti, 2010)). In adult mice, these isoforms seem to have a uniform distribution all along the stereocilia, except at the tip, where some authors found higher expression of γ- actin than β- actin (Furness et al., 2005; Patrinostro et al., 2018). Concerning the cross-section distribution of the isoforms, there are discrepancies in studies between species, it was found that in chick, β- and γ- actin don't have a preferential localization (Höfer et al., 1997), that β- actin is prevalent on the outside of guinea pig stereocilia (Furness et al., 2005) but in mice both isoforms seem to be equally expressed throughout the stereocilium cross-section (Perrin et al., 2010).

When either β- or γ- actin isoform is absent, stereocilia are able to achieve a normal development but later, exhibit premature stereocilia degeneration (Belyantseva et al., 2009; Perrin et al., 2010). This makes sense considering that hearing loss in humans is related to both isoforms, specifically β- actin mutations lead to syndromic types of hearing loss but γ-actin can cause either syndromic or non-syndromic hearing loss (Liu et al., 2008; Morín et

al., 2009; Procaccio et al., 2006; Rendtorff et al., 2006; Rivière et al., 2012; Van Wijk et al., 2003; Zhu et al., 2003).

1.3.2.6 Actin-binding proteins in stereocilia

Stereocilia actin filaments are connected between them by a variety of crosslinkers from the plastin, fascin and espin families, and others. Some of them are Fascins 1, 2 and 3, Plastins 1, 2 and 3, Espin 1, 2A, 2B, 3A, 3B and 4, Filamin B, Actinin 1 and 4, among others. It's been demonstrated that some of these crosslinkers have an essential role for development or maintenance of stereocilia, length and thickness of the bundles and interaction with other structures (reviewed by (Vélez-Ortega & Frolenkov, 2019)).

Some of these proteins have shown changes in their activity with the variation of Ca^{2+} concentrations, some of them are:

- Plastins, which have two Ca^{2+} binding domains (De Arruda et al., 1990).

- Member of gelsolin family, that modify actin dynamics when there is an increase in intracellular Ca^{2+} (Kinosian et al., 1998; Mburu et al., 2010).

- Alpha actinins have a Ca^{2+} binding domain and actinin 1 and actinin 4 whose actin-binding activity is regulated by Ca^{2+} (Burridge & Feramisco, 1981; Tang et al., 2001).

There are also some proteins located at the tips of stereocilia that have capping activity in the plus end of actin like EPS8, EPS8L2, twinfilin 2, CAPZB2, Gelsolin, among others. This proteins by themselves have shown to have roles in processes like stereocilia elongation and growth inhibition when the maximum height of the bundle is achieved (reviewed by (Vélez-Ortega & Frolenkov, 2019)).

Actin filaments also act as cellular tracks for myosin, a cytoskeletal molecular motor. This means that the interaction between these two molecules generates movement and forces depending on the load bound to myosin (Houdusse & Sweeney, 2016). It is to note that myosin is also a Ca^{2+} sensitive protein (Somlyo & Somlyo, 2003).

Specifically myosin XVA seems to have a role in the stereocilia growing process since mutations in its motor domain lead to deafness and short stereocilia (Belyantseva et al., 2003; Beyer et al., 2000; Probst et al., 1998). Another important role of myosin XVA is how it delivers other actin binding proteins to the tips of stereocilia like EPS8 (Manor et al., 2011).

1.3.2.7 Immunostaining

Immunostaining, also called immunolabeling, is a process where a specific antigen is detected using a specific antibody. The success of this technique relies on the specificity of the antibody to target the antigen. This process can be done in two different ways (Figure 6):

- Directly, where the chosen antibody is conjugated to an enzyme or a fluorophore.
- Indirectly, where the primary antibody binds to the antigen and then, one or two labeled secondary antibodies bind to the primary antibody.

Direct detection is better for experiments with antigens that are highly expressed while indirect detection works better when antigens are not highly expressed because in this method more than one molecule of the secondary reagent can bind to the primary antibody which enhances the signal (Abcam, n.d.).

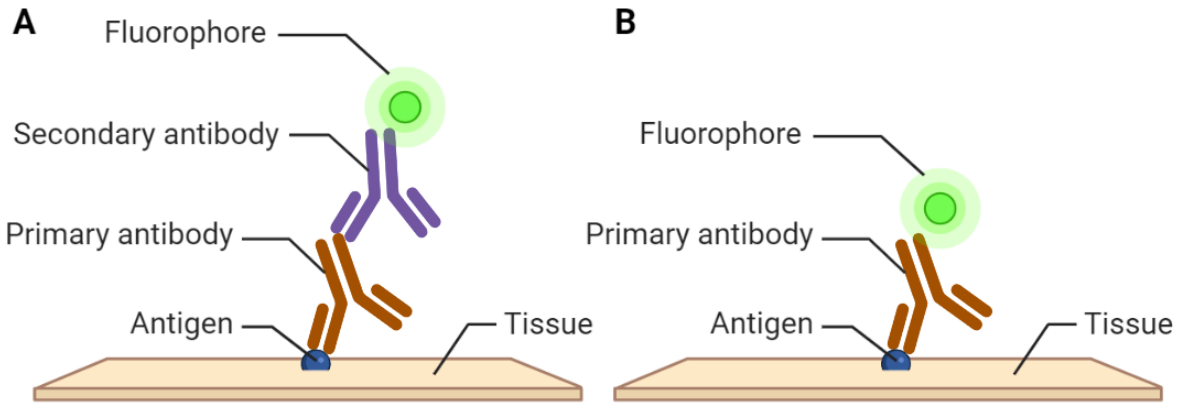

Figure 6: Difference between indirect labeling (A) and direct labeling (B). Image created with Biorender.

1.3.2.8 Confocal Imaging

According to the Leica Microsystems website (Borlinghaus, 2017), confocal microscopes enable optically separated slices of a 3D sample to be recorded as pictures. Ideally, the slices should only cover the depth of focus created in the microscope.

Considering that traditional light sources have a large extension and are not spot-shaped, the light source is projected into a tiny aperture, the pinhole, which acts as a spot-shaped source. The sensor must behave in a similar way on the detector. That is, the sensing region should always coincide with the illumination point and be a spot. The emission light is sent

via a tiny aperture, the detection pinhole, before being recorded by a sensor. When we talk about the "pinhole" in a confocal microscope, we usually mean this detection pinhole.

The term "confocal" refers to the precise configuration in which both illumination and detection are focused on the same point.

The detection pinhole eliminates the light emission that does not come from the focal plane of interest; therefore it is usually called a spatial filter. Figure 7 shows how the pinhole (Ph) blocks the extra focal light (on purple) and just the light emitted from the focal plane (on red) reaches the detector (det)

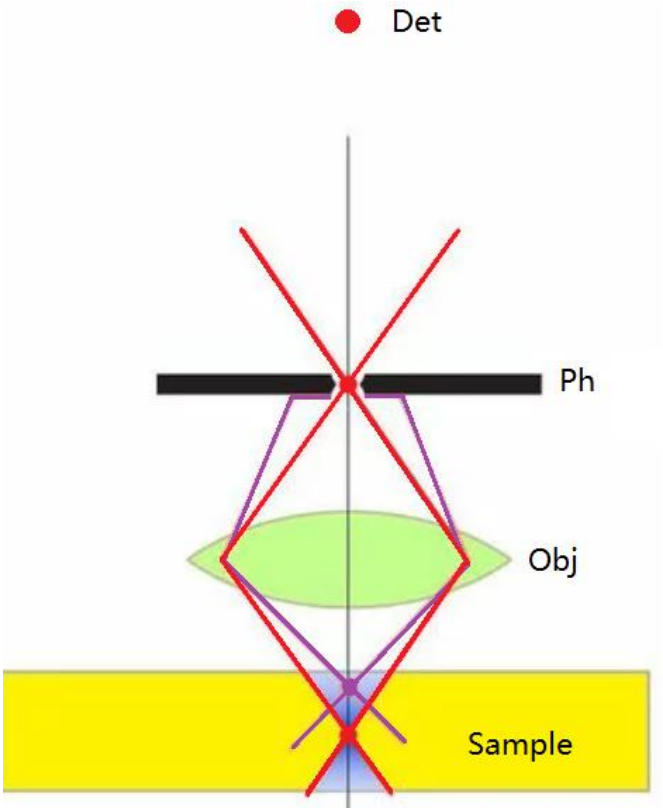

Figure 7: Diagram illustrating how light generated at different planes within the sample is either collected or blocked by the pinhole (Ph) of the confocal microscope. Modified from (Borlinghaus, 2017).

2 METHODOLOGY

2.1 ALGORITHM DESIGN

The algorithm was developed in FIJI (ImageJ version 1.53c) a free software for image visualization and analysis. In a general sense, the approaching strategy was:

1. 3D reconstruction: The confocal microscope gives information in stacks, meaning a sequence of slices of a 3D sample. In order to visualize all the information in a 3D space, these slices were taken back to a 3D figure by putting them together.

2. Stereocilium isolation and information gathering along the stereocilium length: With a z stack, its crucial to guarantee that the information that its being taken is just from the stereocilium, this was achieved by checking on each slice that the selected area corresponded only to the stereocilium of interest.

3. Measure channel intensity (red vs green): Actin isoforms were differentiated by staining with different fluorophores (red for β-actin and green for γ- actin). For the designated area, the information from each channel was obtained using pixel intensity measurements.

2.2 COCHLEA DISSECTION

Organ of Corti explants were isolated from wild-type mice at postnatal day 4 (P4) through postnatal day 6 (P6) depending on the stage of the experiment. This was carried out according to the standard protocols “Mouse Dissection Procedure” and “Neonatal Cochlea Dissection Procedure” from the Velez Laboratory.

Briefly, the mouse is decapitated and subsequently the skull is separated from the skin. Then the skull needs to be separated in halves, being careful of keeping all the auditory structures intact.

Next, the following steps were performed under a Leica Stereo microscope (S9i) (Leica Microsystems, Wetzlar, Germany):

- Remove the brain from the skull
- Locate the cochlea and remove all the adjacent tissue
- Remove the bone around the cochlea
- Separate the cochlea from the tissue that is still attached to its base
- Grab the modiolus at the base and uncoil the cochlear epithelium
- Separate the stria vascularis from the organ of Corti

For extra detail on the procedures see annexes 3 and 4.

If the tissue being dissected was meant to be used in culture, the dissection was performed in a biosafety cabinet class ll type A2 to ensure aseptic conditions as possible. All animal procedures were approved by the Institutional Animal Care and Use Committee (IACUC) at the University of Kentucky (Protocol 2020-3535) (See annex 1) and also reviewed by EIA University ethical committee (See annex 2).

2.3 CELL CULTURE

The explants were held by two glass fibers in Petri dishes (Figure 8) and then they were cultured at 37˚C and 5% CO_2 in Dulbecco's modified Eagle's Medium (DMEM) (Gibco-Thermo Fisher Scientific, MA, US) supplemented with 7% fetal bovine serum (FBS) (Atlanta biologicals, GA, US) and 10 µg/mL ampicillin (Calbiochem-Millipore Sigma, CA, US).

At the end of the culture period (5h and 24h for the cultures with the blocker and 48h for evaluating culture effects on the tissue), the tectorial membrane was removed and the tissue was fixed (as described in section 2.4). For the 24h cultures, fibrous materials produced by the cells were removed (with a suction pipette mounted on a micromanipulator) before tissue fixation.

Cell culture dishes were made with two thin glass fibers pulled from borosilicate glass using a P-2000 puller (Sutter instrument, CA, US) and glued to a Petri dish using Sylgard (Dow, MI, US). The dishes were sterilized before the cell culture through exposure to UV light and ozone in a CoolCLAVE Plus Sterilizer (Amsbio, Abingdon, UK).

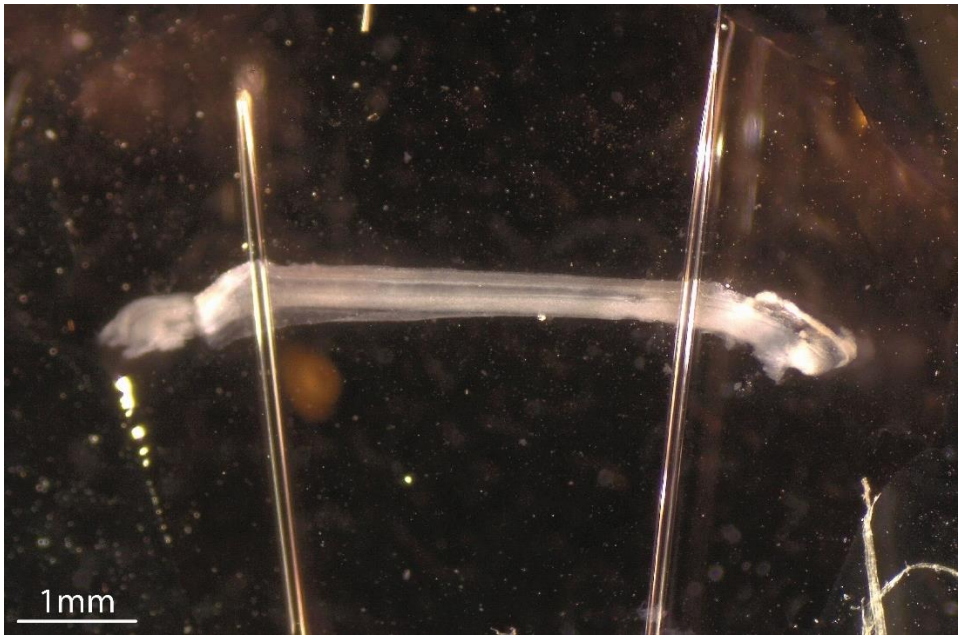

Figure 8: Cochlear tissue on a culture dish, held by two glass fibers. Image acquired using a Leica Stereo microscope (S9i).

2.4 IMMUNOLABELING

The followed protocol for the specific staining of β-actin and γ- actin was:

1. Fix the tissue overnight in 1 ml of 4% paraformaldehyde (PFA) (Electron Microscopy Sciences, PA, US) in 1X PBS (Gibco-Thermo Fisher Scientific, MA, US) at 4°C, in a 7 ml glass scintillation vial.

2. Rinse the tissue in ~5 ml of 1X PBS in a plastic Petri dish.

3. Incubate for 1 hour with 1 ml of methanol (Electron Microscopy Sciences, PA, US) at room temperature in a new 7 ml glass scintillation vial.

4. Remove the methanol and wash the tissue with 1ml of 1X PBS for 5 min. Repeat twice.

5. Permeabilize the tissue in 1ml of 0.5% Triton-X (Electron Microscopy Sciences, PA, US) in 1X PBS during 1h at room temperature in a dark place.

6. Incubate the tissue with a previously prepared mix of 0.5 ml of 0.5% Triton-X and 0.5 ml of 10% normal goat serum (NGS) (Invitrogen-Thermo Fisher Scientific, MA, US) during 3h at 37°C in 1X PBS.

7. Half an hour before the 3h incubation ends, the antibodies need to be labeled following these steps in a dark room since the reagents are light sensitive.

    a. Take two 2 ml Eppendorf tubes.

    b. Add 1 µl of Anti-Beta Actin antibody (mouse monoclonal, clone AC-15, ab6276) (Abcam, Cambridge, UK) to the first tube and 1 µl of Anti-Gamma-Actin/ACRG1 (mouse monoclonal, clone 2A3, MABT824) (Millipore Sigma, MA, US) to the second tube.

    c. Add 5 µl of Zenon Alexa Fluor 555 mouse IgG1 labeling reagent (Invitrogen-Thermo Fisher Scientific, MA, US) to the first tube and 5 µl of Zenon Alexa Fluor 488 mouse IgG2b labeling reagent (Invitrogen-Thermo Fisher Scientific, MA, US) to the second tube.

    d. Mix each tube and wait 5 min in a dark place at room temperature.

    e. Add 5 µl of Zenon blocking reagent (mouse IgG) (Invitrogen-Thermo Fisher Scientific, MA, US) to each of the tubes.

    f. Mix each tube and wait 5 min in a dark place at room temperature.

g. Take the solution from one tube and mix it with the other one. It will result in a total volume of 22 µl.

h. Add 228 µl of 10% NGS in 1X PBS to complete a 250 µl volume. This results in a final concentration for each antibody of 1:250.

8. Remove the NGS-Triton-X solution mix, leaving only the tissue in the scintillation glass vial, and add the antibodies' solution. Incubate overnight at room temperature in a dark place. Keep the vials tilted to guarantee the tissue is fully immersed in the 250 µl antibody solution.

The staining used antibodies directly labeled with fluorophores to avoid inaccurate patterns of β- or γ-actin localization (Perrin et al., 2010). This is likely because of the size of the complex generated in secondary labeling (bigger than in direct labeling, see figure 6) which could lead to penetration problems when trying to get inside the tightly packed actin core.

Of note, the antibodies used in this project had previously been shown to either not cross-react between isoforms (Chaponnier & Gabbiani, 2016; Dugina et al., 2009) and/or used for the immunolabeling of mouse auditory hair cell stereocilia (Patrinostro 2018; Furness 2005; Perrin 2010).

2.5 MOUNTING

Samples were rinsed twice with 1x PBS during 30 min each time. Then, they were placed on glass slides (25 x 75 x 1 mm) (VWR International, PA, US), and it was verified that they were resting on the right side (with the hair cells on top). All the liquid was removed and then a drop of Prolong Diamond Antifade Mountant Media (Invitrogen-Thermo Fisher Scientific, MA, US) was put on top of the tissue to finally be covered with the glass coverslip (22 x 22 x 0.17-0.25 mm) (VWR International, PA, US) (Figure 9). The slides were left overnight for the media to cure. 24 hours later, clear nail polish was used to seal the edges between the coverslip and the glass slide for long term storage.

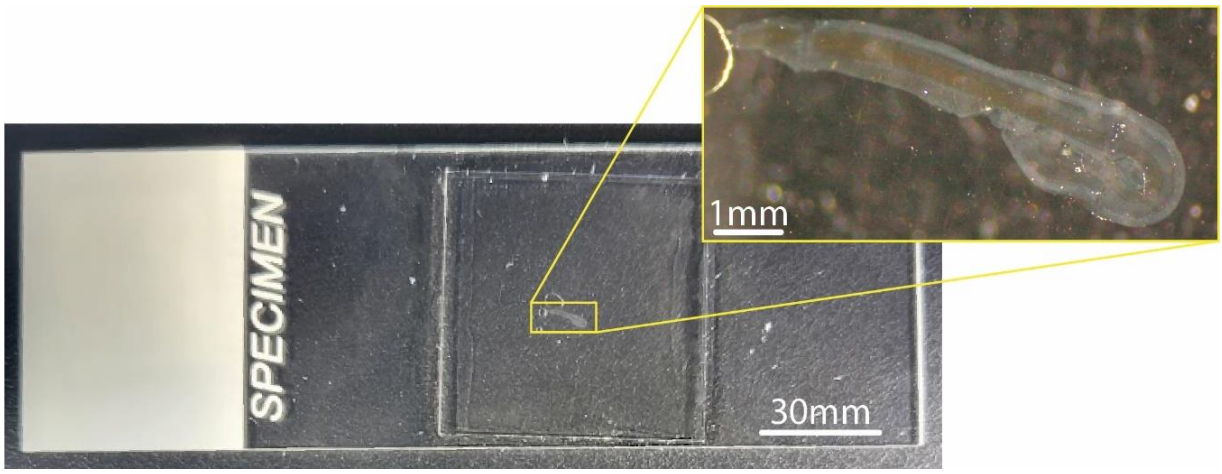

Figure 9: Tissue mounted on the glass slide. The yellow region shows a magnification of the tissue. Images were acquired using a Leica Stereo microscope (S9i).

2.6 CONFOCAL AND BRIGHT FIELD IMAGING

In order to acquire the images, a system for laser confocal imaging was used. This system is based on a Leica SP8 spectral confocal unit (with highly efficient spectral separation with 1 nm precision) on a DM8 CS 5 upright microscope equipped with a HCX PL APO 100X (1.44 NA) and a HC PL APO 10X (0.40 NA) objectives, a motorized stage (for high-precision imaging stitching), four laser lines (405, 488, 552 and 638 nm), a PMT detector and two HyD detectors for super-sensitive photon detection, and the LAS X software (Leica Microsystems, Wetzlar, Germany).

The 10x objective was used to obtain a bright field picture of the entire tissue and find the region of interest, the middle of the organ of Corti (Figure 10).

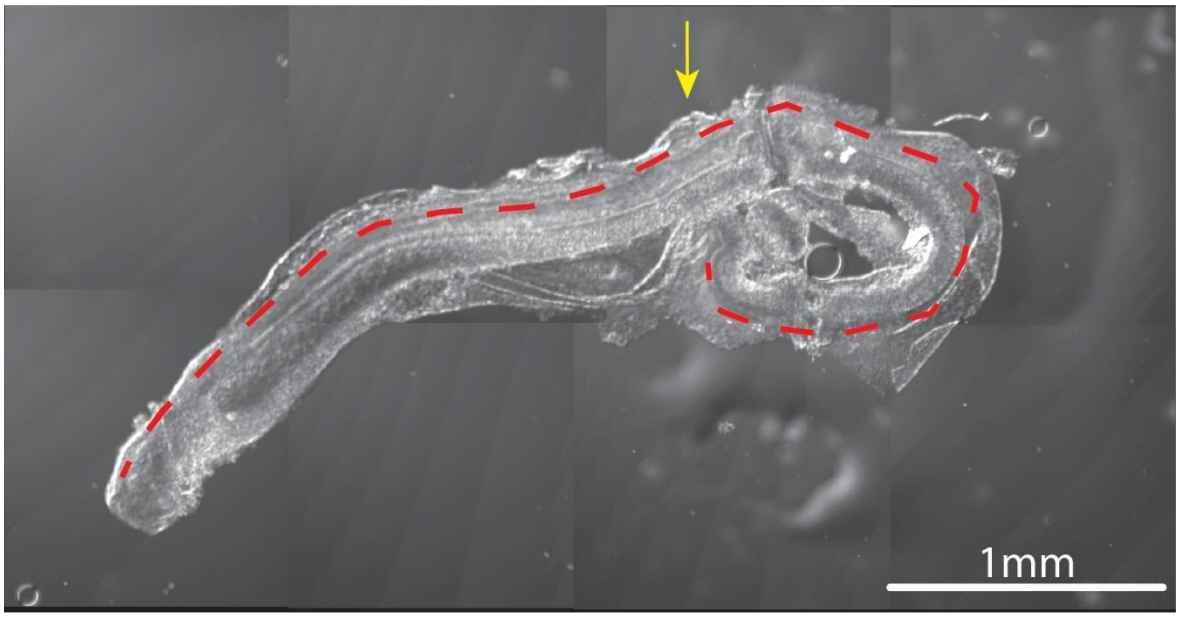

Figure 10: Bright field picture obtained with 10x objective. Dotted line shows where the hair cells are located and the arrow points to the region of interest, the middle of the organ of Corti.

The 100x objective was used to obtain the fluorescent images of the cells at high resolution. For each sample, inner hair cells and third row outer hair cells were imaged. The third row of outer hair cells was chosen because this row is known to exhibit the largest changes in stereocilia morphology after variations in mechanotransduction activity (Vélez-Ortega et al., 2017). For each cell type, between 6 and 9 cells were imaged.

All the images were acquired with a pixel size of 28.41 nm using a pinhole of 0.4 A.U. (Airy Units).

2.7 COMPARISON BETWEEN FRESH TISSUE VS CULTURED TISSUE

Explants from P4 mice were cultured as previously described for two days (P4+48h) and fixed for immunolabeling against both β- and γ- actin. Confocal imaging was performed, and the results were compared with fresh explants from P6 (P6+0h) and P4 (P4+0h) mice from the same litter and with the same immunolabeling procedure. Since these last two were not cultured, the tectorial membrane was removed right before fixing for the immunolabeling. The immunolabeling procedure was performed in parallel for all 3 samples.

2.8 MET CHANNELS BLOCKAGE

Freshly isolated explants were cultured as described in the section 2.3 but with the addition of tubocurarine (60 µM) (Millipore Sigma, MA,US) in the media, for 5 or 24 hours. This concentration of tubocurarine has been shown to block about 90% of the MET current in auditory hair cells from turtle (Farris et al., 2004), and the effects of a 80-90% block in MET current on the morphology of mouse auditory hair cell stereocilia were previously characterized by Vélez-Ortega et al. (2017).

After the culture in control conditions or in the presence of tubocurarine, the samples were fixed, immunolabeled, mounted, and confocal imaged as described above.

2.9 SCANNING ELECTRON MICROSCOPY (SEM)

The explants were cultured as described in section 2.8 for 5 h. At the end of the culture time, the tissue was fixed overnight in 3% each Formaldehyde/Glutaraldehyde (Electron Microscopy Sciences, PA, US) supplemented with 2 mM of $CaCl_2$ (Sigma Aldrich, MO, US).

The samples were rinsed with distilled water and dehydrated with a series of ethanol steps (5, 10, 20, 40, 60, 80 and 100% steps, for 20 min per step), critical point dried from liquid CO_2 using an EM CPD300 automated machine (Leica Microsystems, Wetzlar, Germany), mounted on carbon tape on aluminum cylindrical specimen mounts (Ted Pella, CA, US), coated with a 5 nm layer of platinum using a EMS 150T ES sputter coater (Electron Microscopy Sciences, PA, US) and finally imaged using a dual beam Helios Nanolab 660 microscope (FEI).

2.10 DATA ANALYSIS

All the images obtained were measured and processed with the created algorithm on FIJI (Image J).

The statistical analysis was done with Microsoft Excel and Graph Pad Prism (version 9.2.0) using a two-way ANOVA with matched data points per stereocilium (position from tip to base) and culturing conditions or ages as factors for comparison. All the data shown in the graphs is a summary displayed as mean +/- standard deviation.

The 3D representations for explaining the procedures were designed on Siemens Solid Edge (version 2019).

The figures were designed on Adobe Illustrator unless stated otherwise.

3 RESULTS AND DISCUSSION

3.1 CONFOCAL IMAGING

This small section is an explanation on how the confocal microscope gives the images for a proper understanding on how the figures and the information are displayed in this document.

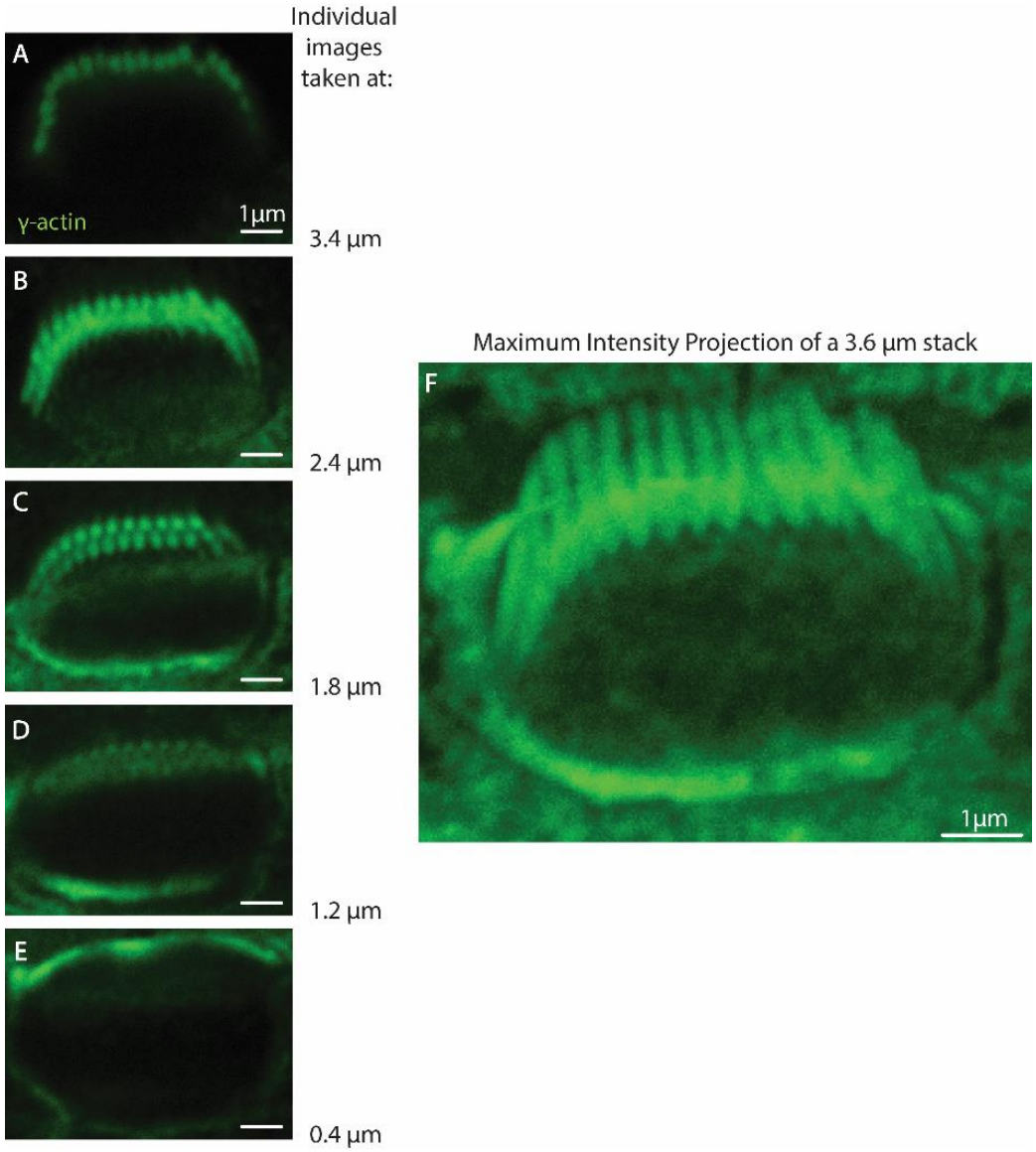

Figure 11: Illustrative images of the data given by the confocal microscope. (A-E) Some slices from a representative z-stack of an inner hair cell stereocilia bundle from the tips of

stereocilia (A) until the cuticular plate (E). (F) Maximum intensity projection of the same confocal stack.

The samples imaged in this project were real cells with a 3D topography. In order to image this volume, the confocal creates a z-stack, which is an arrangement of images that are slices of the 3D object. All the images (slices) within a z-stack in this project were taken 0.2 µm apart from each other.

To get a 2D projection of the 3D object, a compilation of all the images was done. For these results a maximum intensity projection (In ImageJ, Image > stacks > z project > maximum intensity) was obtained as shown in figure 11F. A maximum intensity projection means that the software finds for each pixel in the 2D image, the maximum value across the whole stack so that the final image is a 2D representation of the brightest spots of the stack.

3.2 ALGORITHM

Following the general strategy mentioned in the section 2.1, two approaches were proposed.

The first approach directly used the slices from the stack that the microscope gives. The steps were:

1. Choose 5 images from the stack, each of these images should match one of the chosen regions: tip, tip-middle, middle, middle-bottom and insertion on the cuticular plate. Figure 12A shows the ideal scenario when choosing the regions.

2. On each of the images, draw a circular region that is completely inside of the part of the stereocilium that is being displayed on that specific slide. Figures 12B and 12C show how the circle matches the shape of the stereocilium.

3. Measure the selected region to obtain the average intensity of fluorescence. The measurement needs to be done for both channels (Figure 12D).

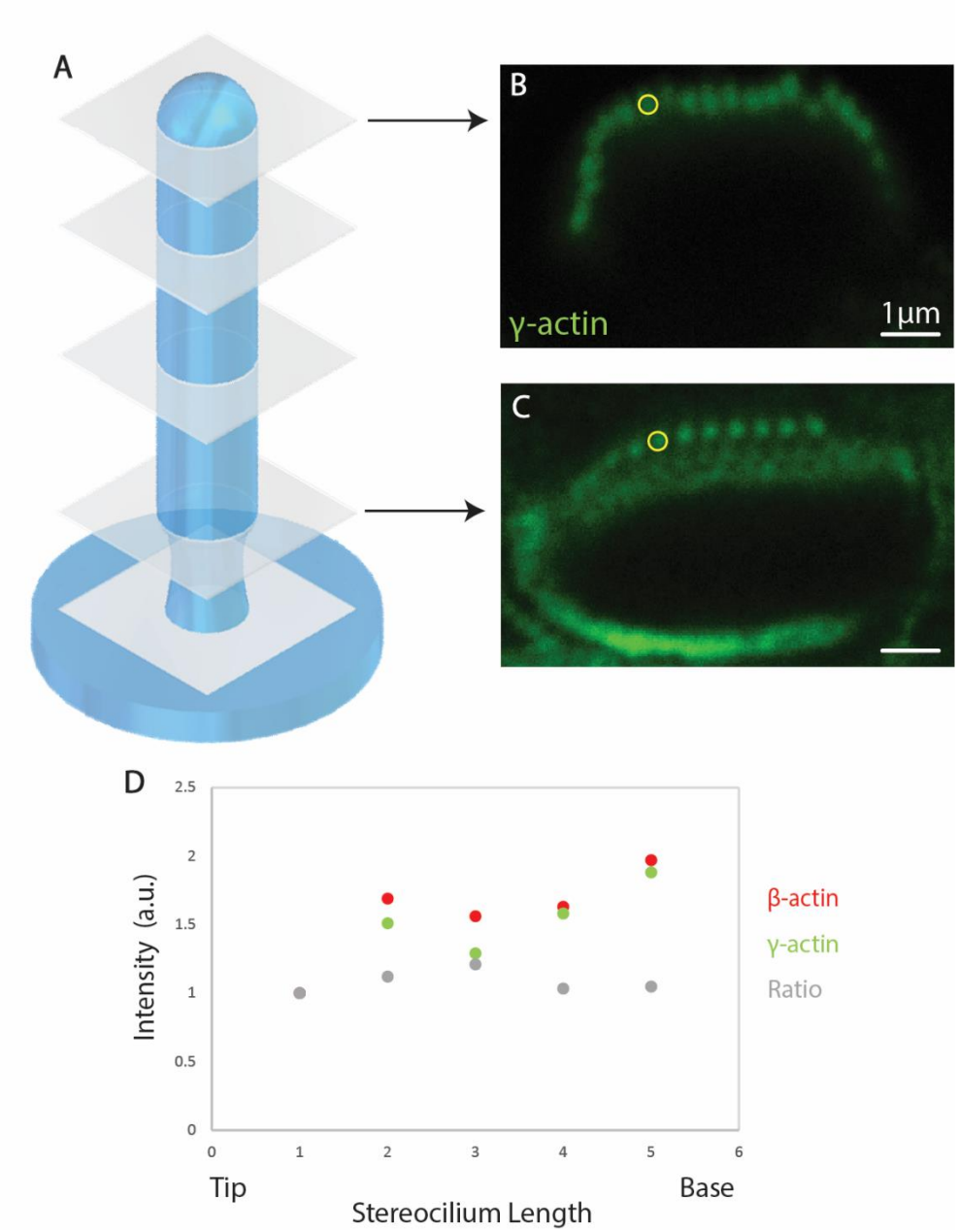

Figure 12: Strategy to quantify fluorescence along stereocilia lengths using the first algorithm. (A) Diagram indicating the 5 planes where stereocilia measurements were performed. (B and C) Representative images showing two positions along the stereocilia length and the regions (yellow circles) used to quantify fluorescence within an individual stereocilium. (D) Obtained data from the quantification in the five regions for both channels and the γ/β ratio.

The second approach used a new cross section obtained after re-slicing the stack. The steps were:

1. Draw a 5-pixel thick line across the entire length of the stereocilium. This needs to be done across the entire set of images of the z-stack to make sure that the line matches the stereocilium (Figure 13A-D).

2. Use the line to reslice the stack (In ImageJ, Image > Stacks > Reslice). The new cross section that is obtained is shown in Figures 13E and 13F.

3. Make another 5-pixel thick line across the stereocilium on the cross section that was obtained from the reslice (Figures 13H, 13I-K)

4. Measure the intensity across the line with a plot profile (In ImageJ, Analyze > plot profile). The measurement needs to be done for both channels with the same line. The obtained data is the average of a prism with sides of 5 pixels x 5 pixels x length of the stereocilium, which corresponds to 142.05 nm x 1142.05 nm x length of the stereocilium (Figures 13L and 13M).

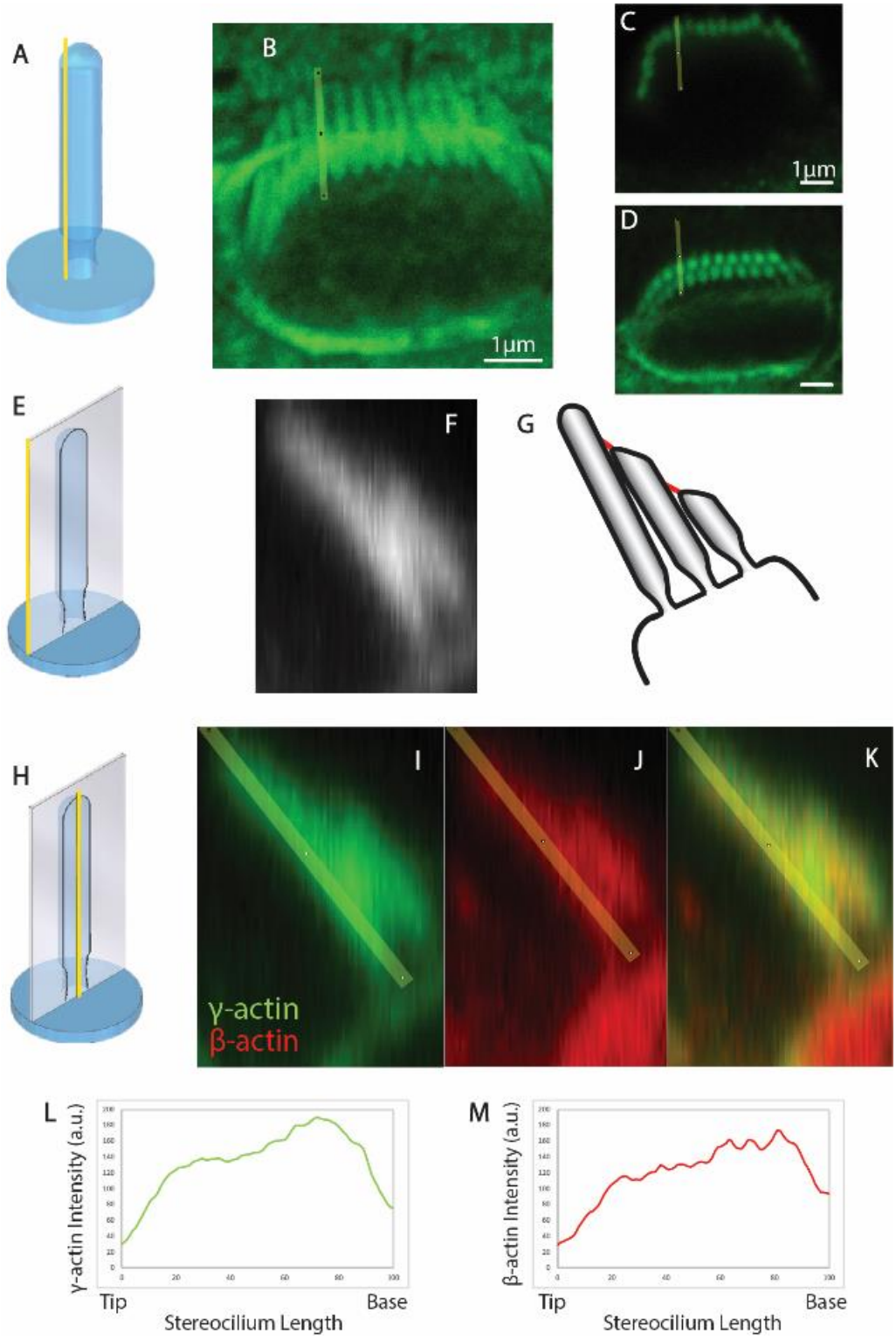

Figure 13: Strategy to quantify fluorescence along stereocilia lengths using the second algorithm. (A,E and H) 3D cartoon representations of the algorithm steps. (B) Line across an individual stereocilium in the maximum-intensity projection image. (C and D) Representative images showing the line in two positions across the stack: near the stereocilia tips (C) and in the middle of the stereocilia shaft (D). (F) Cross section obtained after re-slicing the stack using the line shown in C-D. Two stereocilia are clearly differentiated, one from the tallest row (left) and one from the middle row (right). (G) Cartoon illustrating the orientation of the stereocilia bundle in the cross section shown in F. The stereocilium from the shortest row is too small to be easily resolved by fluorescence microscopy. (I-K) Line across the stereocilia to measure intensity for channel one (I) and channel two (J), and merged image showing the relative fluorescence of both channels (K). (L and M) Obtained data from the quantification along the stereocilium length for each channel.

After getting the two methods and using them on the same set of images to compare the obtained data, it was decided that the second method was better due to the amount of information gathered since this method gives an intensity value for each pixel along the line (Figure 13 L-M) meanwhile the first method just gave five values (Figure 12D). In addition, the second method consumed less time since just two lines and two measurements (one for each channel) needed to be done instead of five regions and ten measurements (one for each region on each channel).

This method was successful for measuring stereocilia in inner hair cells but when it was used for outer hair cells the quantification could not be done. After following the steps, the obtained cross section (Figure 14D) was not understandable enough to draw the second line, the difference between row one and row two of stereocilia was not clear. This makes sense considering that the limits for confocal imaging are around 180 nm laterally and 500 nm axially when the equipment is optimally used (Fouquet et al., 2015) and the diameter of outer hair cells stereocilia is around 150 nm (Hadi et al., 2020) so these structures are on the borderline of the resolution.

Keeping in mind this restriction for the quantification, all the analysis for outer hair cells was done qualitatively based on how the images looked like. To perform quantifications of outer hair cells stereocilia using data obtained with traditional confocal microscopy, a new algorithm would have to be created and tested. The new algorithm could include improvements during the image acquisition (*e.g.*, decreasing the pinhole size, increasing frame averages, increasing image resolution by decreasing pixel size), and/or additional image post-processing techniques (*e.g.,* fluorescence deconvolution). Alternatively, stereocilia from outer hair cells could be imaged using super-resolution techniques like Stochastic Optical Reconstruction Microscopy (STORM), Stimulated Emission Depletion (STED) Microscopy or Structured Illumination Microscopy (SIM). These super-resolution techniques would allow for better separation of individual stereocilia.

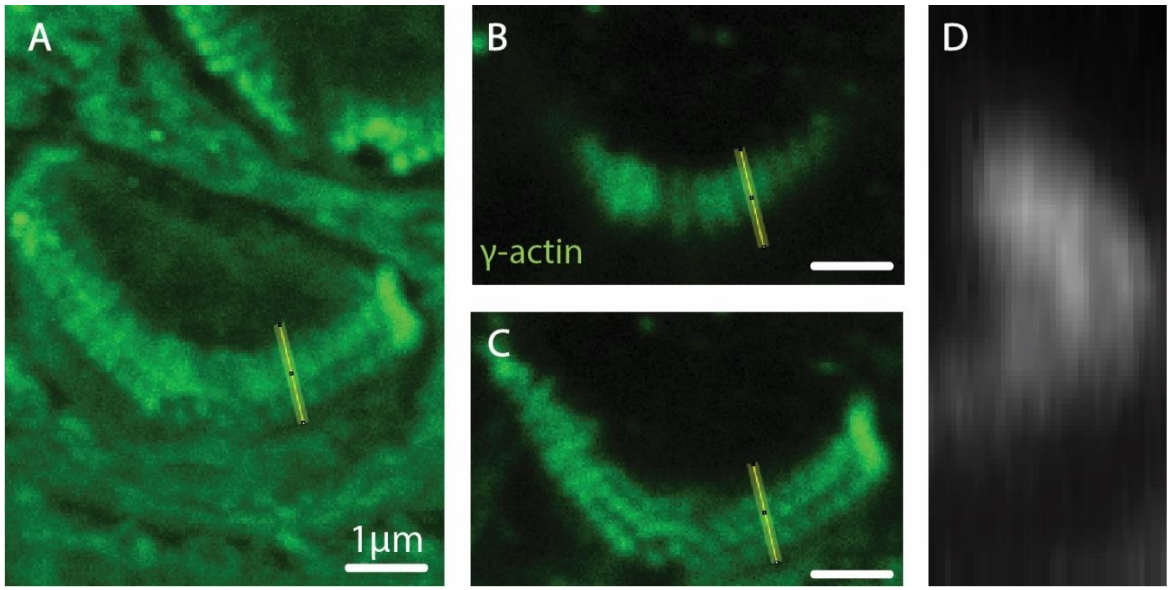

Figure 14: Difficulties measuring outer hair cells with strategy two. (A) Line across the maximum intensity projection. (B and C). Representative images showing the line in two positions across the stack. (D) Obtained cross section where separation between stereocilia rows is difficult.

After gathering all measurements, it was required to compare the obtained values from different stereocilia, different cells and different samples. This comparison cannot be done using raw data values considering that:

- Stereocilia have slightly different lengths.

- Immunostaining is a variable process that relies on the penetration of the antibody, the antibody binding to the structure, the amount of bound antibody, among others. All these variables lead to differences in staining intensity between samples.

- Getting the best quality image requires the adjustment of microscope settings before taking every image. Parameters like the laser intensity and detector gain are varied every time and this generates different intensities between images.

To overcome these drawbacks and considering that the interest of this study is to compare ratios, not absolute values, the data was normalized in this way:

- Length normalization: Stereocilia length is given by the program in pixels. To compare the distribution across the regions of the structure, all the lengths were normalized from 0 (stereocilium tip) to 100% (stereocilium base). This allows to compare relative positions along the stereocilium length.

- Intensity normalization: The microscope used generated 8-bit images, thus the intensity values for each pixel are given as a number from 0 to 255. To compare dark images to bright images, the values were normalized from 1 to 2. This allows to compare the brightest spot from one image to another no matter what the original value was.

With the normalized data the next step was to obtain ratios. Intensities for γ- actin (channel 1-green) were divided over intensities for β- actin (channel 2-red). To interpret these results, it can be said that:

- Ratio<1 means that for that specific point there is an enrichment in β- actin.

- Ratio=1 means that for that specific point there is no particular enrichment of either actin isoform.

- Ratio>1 means that for that specific point there is an enrichment in γ-actin.

3.3 CULTURED VS FRESHLY ISOLATED TISSUE

In vivo, the hair cells are surrounded by two different extracellular solutions as described in section 1.3.2.3. The hair bundles are exposed to endolymph which has a low calcium concentration, and the basolateral membrane is exposed to perilymph with a calcium concentration 20 to 30 times higher (Bosher & Warren, 1978; Ferrary et al., 1988). Unfortunately, it is not possible to culture hair cells in conditions that can replicate their native state with both solutions, it can only be done in extracellular medium that is high in calcium (relative to the endolymph). Therefore, it was questioned whether the ratio between actin isoforms in stereocilia is affected simply by putting the cochlear tissue in culture. Cell culture conditions are required to evaluate the effect of a MET channel blocker on hair cell stereocilia re-arrangements since, currently, there is no way to evaluate this *in vivo*. Therefore, results from this section provided reference values for all samples treated in culture (*in vitro*).

This was evaluated by measuring the relative contribution of both isoforms in three conditions: fresh explants from P4+0 and P6+0 mice and explants from P4 mice that spent two days in culture (P4+2). Samples were immunolabeled, mounted and imaged as described in sections 2.4, 2.5 and 2.6.

In inner hair cells, individual stereocilia were clearly identified from the tallest row (row one) and the middle row (row two) within the hair bundle (Fig. 15A, 15B, 15C). Stereocilia from the shortest row are not easily visualized because their diameter is below the resolution limits of confocal microscopy. Next, the algorithm described in section 3.2 was used to measure the fluorescence intensity along the stereocilia length for β actin (red) and γ actin (green). Measurements for row one showed small but statistically-significant differences between stereocilia at P4+0 and P6+0, but no differences with the cells that spent 48h in

culture conditions (P4+2) (Fig. 15D). The small differences observed between P4+0 and P6+0 could be due to the fact that row one stereocilia are still developing at this age since they continue to grow until ~P16-P18 (Hadi et al., 2020; Kaltenbach et al., 1994). However, cochlear hair cells can only be placed in culture during the first postnatal week since they undergo apoptosis when dissected at later time points.

Row two stereocilia from inner hair cells have fully achieved their maximum height at P4 (Hadi et al., 2020; Kaltenbach et al., 1994; Roth & Bruns, 1992), and they did not show any differences in the ratio of γ actin to β actin between freshly-isolated or culture tissue (Fig. 15E). Nevertheless, a small decrease in the ratio near the stereocilia base was observed which seems to indicate a higher amount of γ actin at the stereocilia tip and higher amount of β actin near the stereocilia base. However, given that the cuticular plate (the actin network where the stereocilia are inserted) is mainly made up of beta actin (Fig. 15A-C) (Furness et al., 2005), the small decrease in γ to β actin ratio near the stereocilia base could be due to small fluorescence spillover from the cuticular plate.

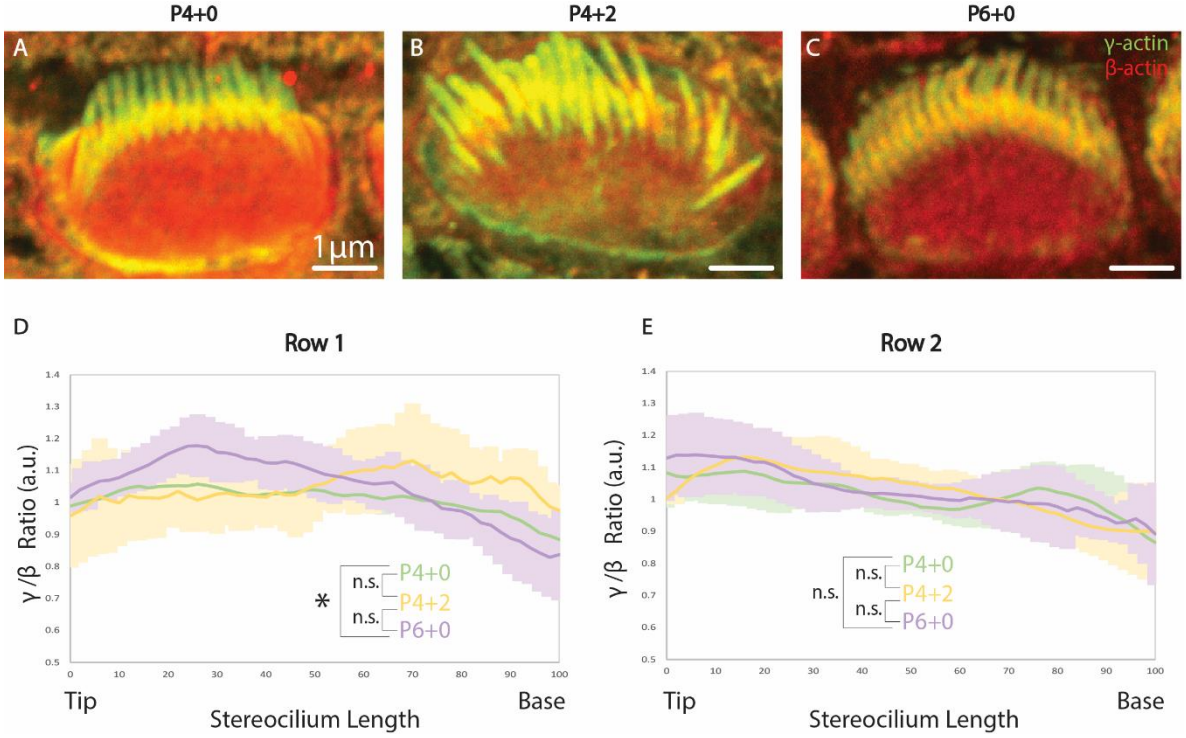

Figure 15: Ratio of gamma to beta actin in freshly-isolated vs. cultured inner hair cell stereocilia. (A-C) Representative confocal images from inner hair cell bundles of freshly-isolated tissue at postnatal day 4 (P4+0) (A) or 6 (P6+0) (C), or of tissue dissected at P4 and cultured for 2 days (P4+2) (B). (D and E) Comparison of the ratios obtained for the mentioned timepoints in stereocilia from row one (tallest) and row two (middle). Data shown

*as mean ± standard deviation for n=15/3 stereocilia/cells per condition. Statistical analysis done by two-way ANOVA, n.s., non-significant, *P<0.05.*

In outer hair cells, individual stereocilia are not easily visualized due to the reasons explained in section 3.2, however, the images seem to show a similar behavior to inner hair cells. Even when it was not possible to quantify intensities for both channels, figure 16 shows the presence of the yellow color in the bundles, which suggests a uniform distribution of both isoforms in the three evaluated conditions.

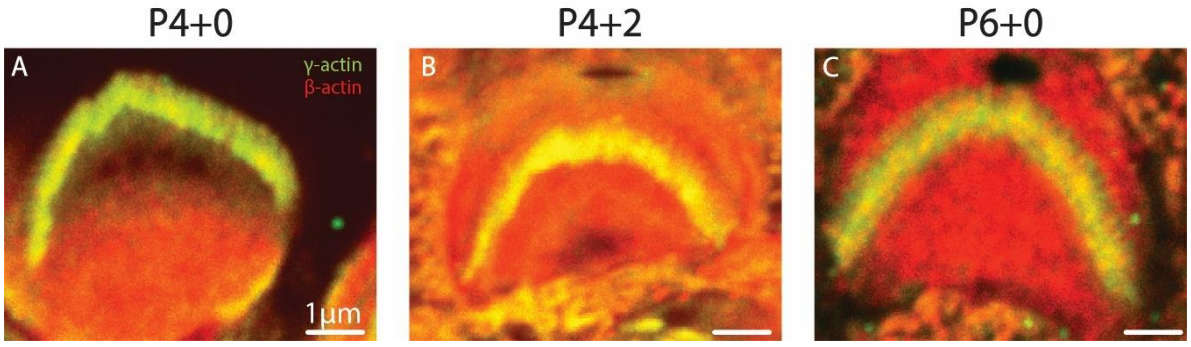

Figure 16: Representative confocal images obtained from outer hair cells bundles of freshly isolated tissue at postnatal day 4 (P4+0) (A) or 6 (P6+0) (C), or of tissue dissected at P4 and cultured for 2 days (P4+2) (B). Images are representative of n = 3 cells/condition.

These findings match with the data published by Perrin et al. (2010) and Patrinostro et al. (2018), where they stated that, in young postnatal mouse hair cells, β and γ actin colocalize along the length of stereocilia. Moreover, as shown in figures 15A-C and 16A-C this colocalization is maintained for both inner and outer hair cells even during culture conditions where calcium concentrations are altered from the ones *in vivo.*

3.4 IMPACT OF A DECREASE IN MET CHANNEL ACTIVITY ON THE CONTRIBUTION OF ACTIN ISOFORMS WITHIN THE STEREOCILIA CYTOSKELETON

After confirming that actin isoforms remain in the same proportions in culture conditions, the next step was to evaluate if these proportions could be affected by a decrease in the calcium entry to the stereocilia.

As an internal control between batches of tubocurarine, a MET channel blocker, and different users of the described protocol, SEM imaging is performed to confirm that the blocker is behaving as previously described by (Vélez-Ortega et al., 2017) who demonstrated that the presence of MET channel blockers (like tubocurarine or benzamil) in the transducing stereocilia generates abnormal thin tips and eventual shrinking. Figure 17 shows an outer hair cell bundle after 5h in culture with the presence of tubocurarine (60µM), the yellow arrows show the appearance of the thin tips, which confirms the action of the blocker and hence, the cytoskeleton remodeling.

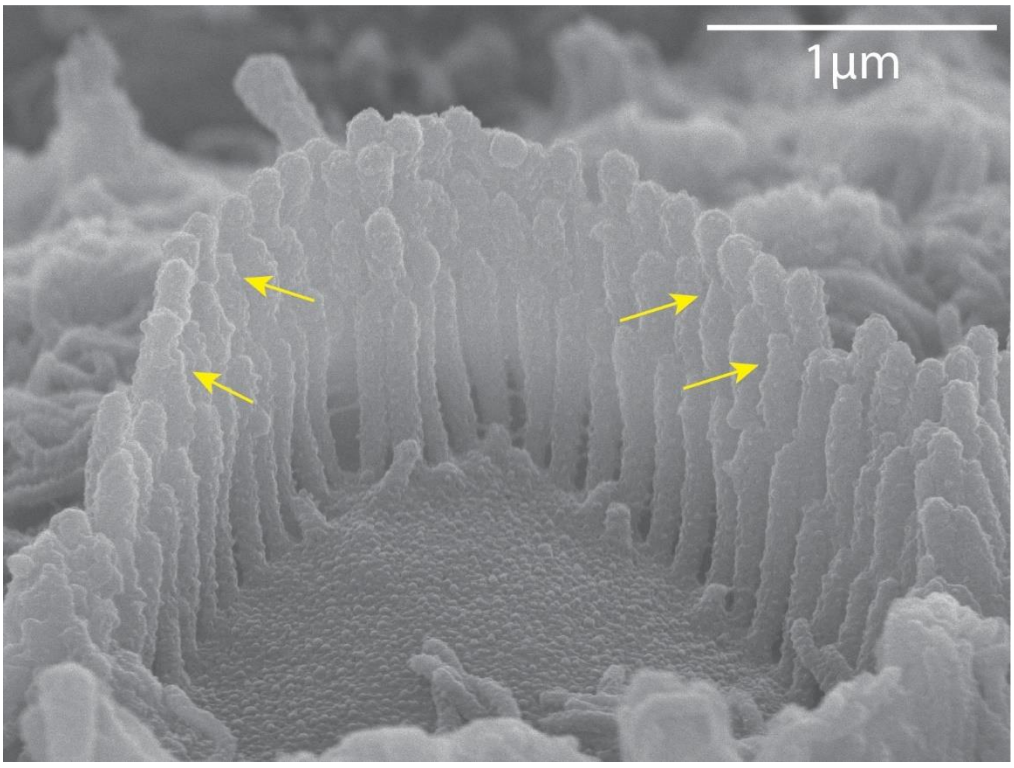

Figure 17: SEM image obtained from an outer hair cell bundle after 5h incubation with 60 µM tubocurarine. Arrows point to some of the second row stereocilia exhibiting MET-dependent stereocilia remodeling (i.e. the thin tips).

Next, to evaluate the effect of a reduction in MET channel activity on the ratio of actin isoforms, explants from P4+0 mice were incubated with the MET channel blocker tubocurarine (60µM) during 5 or 24 hours. Samples were immunolabeled, mounted and imaged as described in sections 2.4, 2.5 and 2.6.

For inner hair cells, the quantification of β actin (red) and γ actin (green) fluorescence intensity along the stereocilia length was done with the algorithm described in section 3.2.

Ratios of γ/β actin within inner hair cells stereocilia after 5h culture showed a small but statistically significant difference between tubocurarine-treated and control samples for row one ($P = 0.0023$), but not for row two (Figure 18). Given that MET channels are located at the tips of row two but not row one stereocilia (Beurg et al., 2009), this result was rather surprising. To confirm this finding, it will be necessary to perform additional series in order to quantify more stereocilia and cells. Once again, differences in row one could be due to the fact that stereocilia in this row are still growing. However, the most important result from these experiments is the fact that no statistically significant differences in the γ/β actin ratio were observed in stereocilia from the mechano-transducing row two after a 5 h reduction in MET channel activity.

After 24h in culture in control conditions or in the presence of the MET channel blocker, no statistically significant differences were observed in the γ/β actin ratios of stereocilia from row one or row two. Once again, indicating that a 24h decrease in MET channel activity did not trigger any changes in the composition of the stereocilia actin core, in spite of any changes in their overall morphology (thickness and/or height).

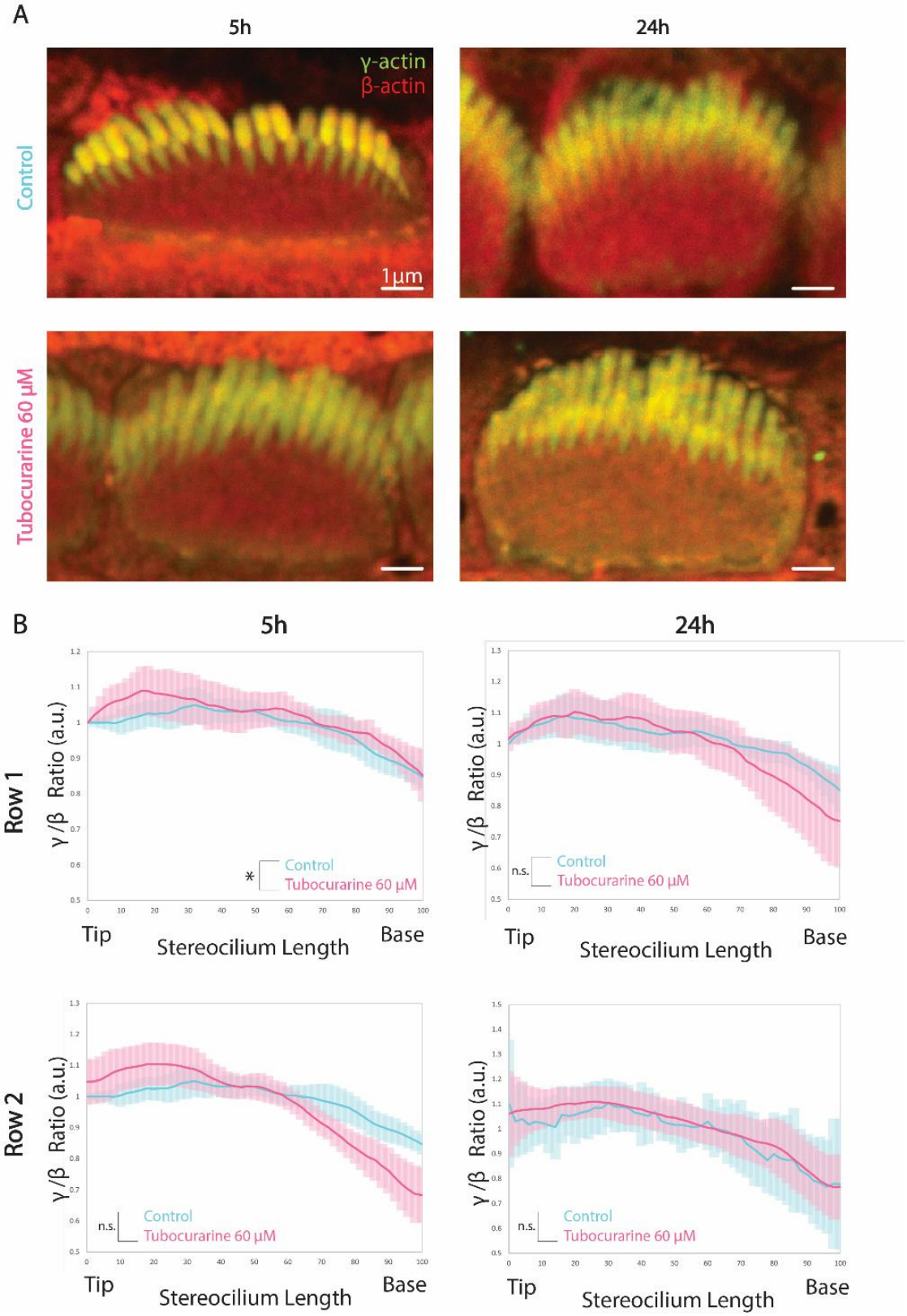

*Figure 18: Ratio of gamma to beta actin in treated vs control inner hair cell stereocilia. (A) Representative confocal images from inner hair cell bundles after normal culture conditions (top) or after incubation with tubocurarine (bottom) during 5h (left) or 24h (right). (B) Comparison of the ratios obtained for the mentioned conditions and timepoints in stereocilia from row one (top) and row 2 (bottom). Data shown as mean ± standard deviation (n = 15/3 stereocilia/cells per condition). Statistical analysis done by two-way ANOVA, n.s., non-significant, *P<0.05.*

Transducing stereocilia from outer hair cells are known to display larger morphological changes after variations in MET channel activity (Vélez-Ortega et al., 2017). However, it was not possible to extract reliable measurements from images of outer hair cells given that the thickness of each stereocilium (~150-200 nm) is near the resolution limits of the confocal microscope (~200 nm). Instead, a qualitative evaluation of the images was performed looking for obvious enrichments of either actin isoform in stereocilia from row one (non mechano-transducing) vs row two (mechano-transducing).

All outer hair cells showed a pattern of colocalization for both actin isoforms in the bundles, and no obvious differences between rows were observed after a decrease in MET channel activity, even though significant stereocilia morphological changes are evident after 5h or 24h (Figure 17, and (Vélez-Ortega et al., 2017)). This colocalization of both actin isoforms can be clearly seen in figure 19 where most of the bundles are yellow. Although some isolated green and red spots are visible, they show no preferential localization patterns restricted to row one or row two, or to a particular culture condition.

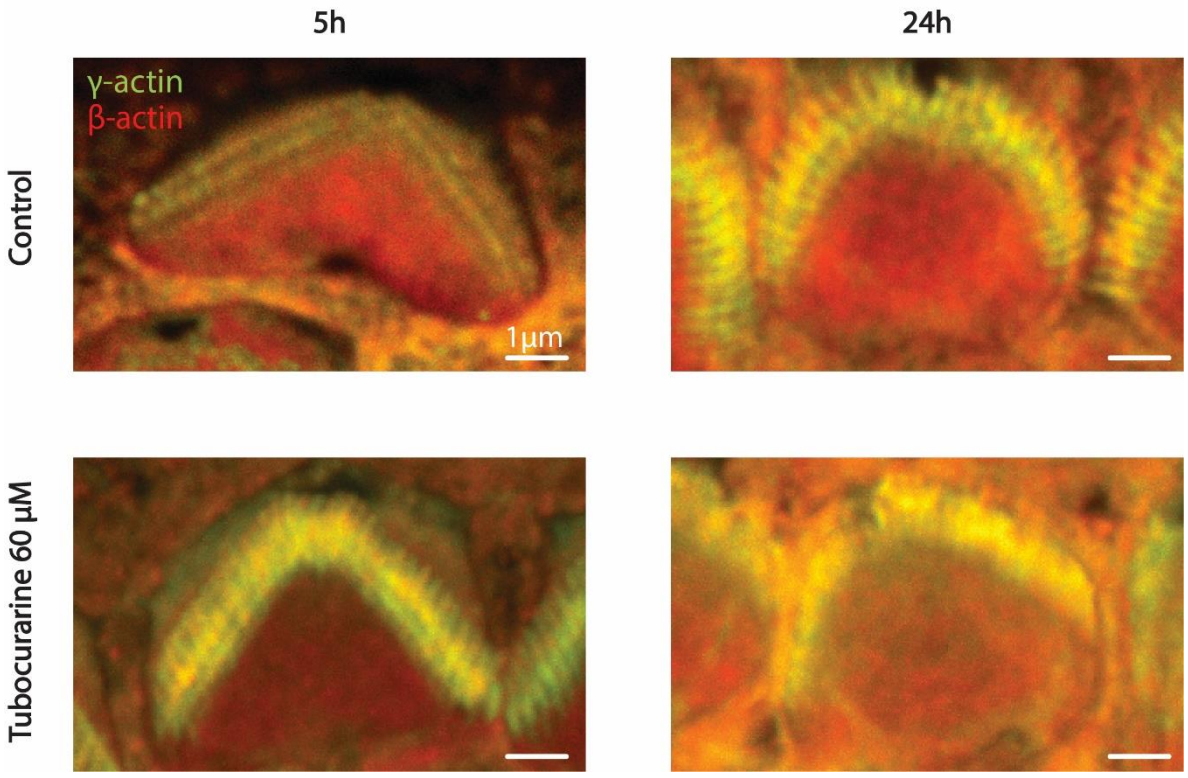

Figure 19: Representative confocal images obtained from outer hair cell bundles for control (top) and tubocurarine-treated (bottom) samples at 5h (left) and 24h (right). Images are representative of n = 15 cells/condition for 5h and n = 18 for 24h.

The obtained data shows that the cytoskeleton rearrangements in stereocilia that occur after a decrease in MET channel activity are not explained by a change in the proportions of β and γ actin since both isoforms seem to colocalize in both control samples and samples treated with a MET channel blocker, for both inner and outer hair cell bundles (Figures 18A and 19). Even if there is some evidence that affirms that β and γ actin have different rates of polymerization and depolymerization when they are bound to calcium (Bergeron et al., 2010), this data was obtained at 25°C while all the experiments in this project were developed at 37°C, this might explain why there is no change in how the isoforms are distributed during the cytoskeleton disassembly driven by the change in calcium concentrations.

Furthermore, as it was previously stated, even if β and γ actin are redundant during the development of stereocilia bundles, both isoforms are required for long lasting stereocilia since the absence of either isoform results in stereocilia degeneration (Belyantseva et al., 2009; Patrinostro et al., 2018; Perrin et al., 2010).

Also, some crosslinkers play an essential role in the lifespan of stereocilia:

Plastin 1 is essential to determine stereocilia dimensions. Mice lacking this protein exhibit shorter and thinner stereocilia. Moreover, this crosslinker was found to regulate the actin filament packing pattern since wildtype mice have “liquid” packing (*i.e.* not in a perfect crystal arrangement) but mutants without Plastin 1 developed stereocilia with a nearly perfect hexagonal actin packing. This change implies that the maximum diameter cannot be reached and that the presence of Plastin 1 allows for a mixture of different crosslinker lengths, which allows the liquid packing (Krey et al., 2016).

Espin is also necessary for the formation and maintenance of the parallel actin core in stereocilia. When espin is absent, abnormally thin and short stereocilia are developed and they eventually degenerate. One of the reasons behind this phenomenon is that espin cross-links are stronger than the ones from fascin when it comes to actin filaments twisting in the actin bundles and since this twisting is likely to reflect a high conformational rigidity, lacking this protein leads to a deterioration in the parallel actin bundle stability (Sekerková et al., 2011).

Having both actin isoforms might allow different actin binding proteins to be present along the length of stereocilia. As it was previously stated, the mixture of different crosslinker proteins generates a heterogeneous pattern in the actin packing. In fact, Winkelman et al. (2016) proposed that filament spacing promotes different actin binding proteins to bind into different actin networks. This means that some bundlers can bind actin only if the spacing between the fibers is appropriate.

Moreover, the twisting of the actin filaments can be controlled by some of its binding proteins. For example, cofilin, a depolymerizing protein, can alter the actin structure by changing its filament twist, as a consequence, binding sites for other proteins can be hidden or moved, inhibiting their binding to actin as it was demonstrated for phalloidin (McGough et al., 1997). Perhaps, changes in the twisting of actin filaments could also impact how myosin motors bind and/or travel along the stereocilia length.

With the presented information, it was hypothesized that the explanation behind the findings displayed in this project could be that both actin isoforms remain in the same proportions as an intrinsic mechanism for either allowing the binding of different families of crosslinkers or for the preservation of the proper actin filament twisting so that all the necessary proteins can bind. Having all the molecular machinery in the cytoskeleton for long lasting and functional stereocilia would be the reason behind both possibilities.

In addition, the mechanism behind the cytoskeleton rearrangements in the presence of MET channels blockers could be related to calcium-dependent conformational changes in calcium sensitive actin crosslinkers considering that, as it was previously explained, some of them are essential for the maintenance of stereocilia. Other calcium-sensitive actin-binding proteins should also be evaluated such as those mentioned in section 1.3.2.6.

4 CONCLUSIONS AND FINAL CONSIDERATIONS

Culturing effects on actin proportions in the stereocilia cytoskeleton were evaluated to guarantee that following results were not culturing artifacts. No significant changes were observed to the ratios of β- and γ- actin isoforms along the lengths of transducing stereocilia up to 48 hours in vitro. Next, MET-dependent changes in the cytoskeleton were measured but no changes in the ratio of β- and γ- actin were observed during the cytoskeleton rearrangements of transducing stereocilia.

Displayed information proves that the stereocilia cytoskeleton maintains the proportions of β- and γ- actin during the MET-dependent remodeling. This demonstrates that the differences between β- and γ- actin regarding their polymerization and depolymerization rates in a Ca^{2+}-dependent way, are not the main mechanism driving stereocilia cytoskeleton rearrangements during changes in intracellular Ca^{2+} concentrations.

As future directions of this project, the presence of some crosslinkers should be evaluated in stereocilia that lacks each of the actin isoforms. Explants from β- and γ- actin knockout mice can be dissected and immunolabeled against the chosen crosslinkers to evaluate if the absence of either actin isoform is related to the absence of any of these crosslinker proteins. Then, electron microscopy images can be done to evaluate changes in the actin filament packing in the absence of actin isoforms.

Following the crosslinkers idea, it would be valuable to evaluate how the blockage of the MET channels affects the presence of calcium sensitive crosslinkers or other actin-binding proteins in stereocilia. The same methods used here could be used with a different quantification and immunolabeling against such proteins. This would answer if the cytoskeleton rearrangements driven by a change in the calcium concentrations in stereocilia are due to calcium-dependent changes in these proteins.

Finally, the influence of MET channel blockage in the actin composition of the cuticular plate should be evaluated in different regions of the organ of Corti since, during the execution of this project, some differences were seen in the actin distribution in the cuticular plate in a region dependent way (data not shown).

REFERENCES

Abcam. (n.d.). *Introduction to immunohistochemistry (IHC)*. Retrieved October 5, 2021, from https://www.abcam.com/kits/introduction-to-immunohistochemistry-ihc

Assad, J. A., Shepherd, G. M. G., & Corey, D. P. (1991). Tip-link integrity and mechanical transduction in vertebrate hair cells. *Neuron*. https://doi.org/10.1016/0896-6273(91)90343-X

Avettand-Fenoël, V., Marlin, S., Vauloup-Fellous, C., Loundon, N., François, M., Couloigner, V., Rouillon, I., Drouin-Garraud, V., Laccourreye, L., Denoyelle, F., Guilleminot, T., Grabar, S., & Leruez-Ville, M. (2013). Congenital cytomegalovirus is the second most frequent cause of bilateral hearing loss in young french children. *Journal of Pediatrics*. https://doi.org/10.1016/j.jpeds.2012.08.009

Belyantseva, I. A., Boger, E. T., & Friedman, T. B. (2003). Myosin XVa localizes to the tips of inner ear sensory cell stereocilia and is essential for staircase formation of the hair bundle. *Proceedings of the National Academy of Sciences of the United States of America*. https://doi.org/10.1073/pnas.2334417100

Belyantseva, I. A., Perrin, B. J., Sonnemann, K. J., Zhu, M., Stepanyan, R., McGee, J., Frolenkov, G. I., Walsh, E. J., Friderici, K. H., Friedman, T. B., & Ervasti, J. M. (2009). γ-Actin is required for cytoskeletal maintenance but not development. *Proceedings of the National Academy of Sciences of the United States of America*. https://doi.org/10.1073/pnas.0900221106

Bergeron, S. E., Zhu, M., Thiem, S. M., Friderici, K. H., & Rubenstein, P. A. (2010). Ion-dependent polymerization differences between mammalian β- and γ-nonmuscle actin isoforms. *Journal of Biological Chemistry*. https://doi.org/10.1074/jbc.M110.110130

Beurg, M., Fettiplace, R., Nam, J. H., & Ricci, A. J. (2009). Localization of inner hair cell mechanotransducer channels using high-speed calcium imaging. *Nature Neuroscience*. https://doi.org/10.1038/nn.2295

Beyer, L. A., Odeh, H., Probst, F. J., Lambert, E. H., Dolan, D. F., Camper, S. A., Kohrman, D. C., & Raphael, Y. (2000). Hair cells in the inner ear of the pirouette and shaker 2 mutant mice. *Journal of Neurocytology*. https://doi.org/10.1023/a:1026515619443

Borlinghaus, R. . (2017). *Pinhole Effect in Confocal Microscopes*. https://www.leica-microsystems.com/science-lab/pinhole-effect-in-confocal-microscopes/

Bosher, S. K., & Warren, R. L. (1978). Very low calcium content of cochlear endolymph, an extracellular fluid. *Nature*. https://doi.org/10.1038/273377a0

Burridge, K., & Feramisco, J. R. (1981). Non-muscle α-actinins are calcium-sensitive actin-binding proteins. *Nature*. https://doi.org/10.1038/294565a0

Caberlotto, E., Michel, V., de Monvel, J. B., & Petit, C. (2011). Coupling of the mechanotransduction machinery and F-actin polymerization in the cochlear hair bundles. *BioArchitecture*. https://doi.org/10.4161/bioa.1.4.17532

Caberlotto, E., Michel, V., Foucher, I., Bahloul, A., Goodyear, R. J., Pepermans, E., Michalski, N., Perfettini, I., Alegria-Prévot, O., Chardenoux, S., Cruzeiro, M. Do, Hardelin, J. P., Richardson, G. P., Avan, P., Weil, D., & Petit, C. (2011). Usher type 1G protein sans is a critical component of the tip-link complex, a structure controlling actin polymerization in stereocilia. *Proceedings of the National Academy of Sciences of the United States of America*. https://doi.org/10.1073/pnas.1017114108

CDC. (2020). *Data and Statistics About Hearing Loss in Children | CDC*. https://www.cdc.gov/ncbddd/hearingloss/data.html

Chaponnier, C., & Gabbiani, G. (2016). Monoclonal antibodies against muscle actin isoforms: Epitope identification and analysis of isoform expression by immunoblot and immunostaining in normal and regenerating skeletal muscle. *F1000Research*. https://doi.org/10.12688/f1000research.8154.1

Corey, D. P., & Hudspeth, A. J. (1979). Ionic basis of the receptor potential in a vertebrate hair cell [12]. In *Nature*. https://doi.org/10.1038/281675a0

De Arruda, M. V., Watson, S., Lin, C. S., Leavitt, J., & Matsudaira, P. (1990). Fimbrin is a homologue of the cytoplasmic phosphoprotein plastin and has domains homologous with calmodulin and actin gelation proteins. *Journal of Cell Biology*. https://doi.org/10.1083/jcb.111.3.1069

DeRosier, D. J., Tilney, L. G., & Egelman, E. (1980). Actin in the inner ear: The remarkable structure of the stereocilium. *Nature*. https://doi.org/10.1038/287291a0

Dillard, L. K., Fullerton, A. M., & McMahon, C. M. (2021). Ototoxic hearing loss from antimalarials: A systematic narrative review. *Travel Medicine and Infectious Disease*. https://doi.org/10.1016/j.tmaid.2021.102117

Ding, N., Lee, S., Lieber-Kotz, M., Yang, J., & Gao, X. (2021). Advances in genome editing for genetic hearing loss. In *Advanced Drug Delivery Reviews*. https://doi.org/10.1016/j.addr.2020.05.001

Drummond, M. C., Belyantseva, I. A., Friderici, K. H., & Friedman, T. B. (2012). Actin in hair cells and hearing loss. In *Hearing Research*. https://doi.org/10.1016/j.heares.2011.12.003

Dugina, V., Zwaenepoel, I., Gabbiani, G., Clément, S., & Chaponnier, C. (2009). β- and γ-cytoplasmic actins display distinct distribution and functional diversity. *Journal of Cell Science*. https://doi.org/10.1242/jcs.041970

Encyclopedia Britannica. (n.d.). *Transmission of sound within the inner ear.* Retrieved October 5, 2021, from https://www.britannica.com/science/ear/Transmission-of-sound-

within-the-inner-ear

Faistauer, M., Lang Silva, A., Félix, T. M., Todeschini de Souza, L., Bohn, R., Selaimen da Costa, S., & Petersen Schmidt Rosito, L. (2021). Etiology of early hearing loss in Brazilian children. *Brazilian Journal of Otorhinolaryngology*. https://doi.org/10.1016/j.bjorl.2021.02.012

Farris, H. E., LeBlanc, C. L., Goswami, J., & Ricci, A. J. (2004). Probing the pore of the auditory hair cell mechanotransducer channel in turtle. *Journal of Physiology*. https://doi.org/10.1113/jphysiol.2004.061267

Ferrary, E., Huy, P. T. B., Roinel, N., Bernard, C., & Amiel, C. (1988). Calcium and the inner ear fluids. *Acta Oto-Laryngologica*. https://doi.org/10.3109/00016488809125130

Fettiplace, R., & Kim, K. X. (2014). The physiology of mechanoelectrical transduction channels in hearing. In *Physiological Reviews*. https://doi.org/10.1152/physrev.00038.2013

Fouquet, C., Gilles, J. F., Heck, N., Santos, M. Dos, Schwartzmann, R., Cannaya, V., Morel, M. P., Davidson, R. S., Trembleau, A., & Bolte, S. (2015). Improving axial resolution in confocal microscopy with new high refractive index mounting media. *PLoS ONE*. https://doi.org/10.1371/journal.pone.0121096

Frolenkov, G. I., Belyantseva, I. A., Friedman, T. B., & Griffith, A. J. (2004). Genetic insights into the morphogenesis of inner ear hair cells. In *Nature Reviews Genetics*. https://doi.org/10.1038/nrg1377

Furness, D. N., Katori, Y., Mahendrasingam, S., & Hackney, C. M. (2005). Differential distribution of β- and γ-actin in guinea-pig cochlear sensory and supporting cells. *Hearing Research*. https://doi.org/10.1016/j.heares.2005.05.006

Furness, David N., & Hackney, C. M. (2006). The Structure and Composition of the Stereociliary Bundle of Vertebrate Hair Cells. In *Vertebrate Hair Cells*. https://doi.org/10.1007/0-387-31706-6_3

Hadi, S., Alexander, A. J., Vélez-Ortega, A. C., & Frolenkov, G. I. (2020). Myosin-XVa Controls Both Staircase Architecture and Diameter Gradation of Stereocilia Rows in the Auditory Hair Cell Bundles. *JARO - Journal of the Association for Research in Otolaryngology*. https://doi.org/10.1007/s10162-020-00745-4

Höfer, D., Ness, W., & Drenckhahn, D. (1997). Sorting of actin isoforms in chicken auditory hair cells. *Journal of Cell Science*. https://doi.org/10.1242/jcs.110.6.765

Houdusse, A., & Sweeney, H. L. (2016). How Myosin Generates Force on Actin Filaments. In *Trends in Biochemical Sciences*. https://doi.org/10.1016/j.tibs.2016.09.006

Kaltenbach, J. A., Falzarano, P. R., & Simpson, T. H. (1994). Postnatal development of the hamster cochlea. II. Growth and differentiation of stereocilia bundles. *Journal of*

Comparative Neurology. https://doi.org/10.1002/cne.903500204

Kawashima, Y., Géléoc, G. S. G., Kurima, K., Labay, V., Lelli, A., Asai, Y., Makishima, T., Wu, D. K., Della Santina, C. C., Holt, J. R., & Griffith, A. J. (2011). Mechanotransduction in mouse inner ear hair cells requires transmembrane channel-like genes. *Journal of Clinical Investigation*. https://doi.org/10.1172/JCI60405

Kinosian, H. J., Newman, J., Lincoln, B., Selden, L. A., Gershman, L. C., & Estes, J. E. (1998). Ca2+ regulation of gelsolin activity: Binding and severing of F-actin. *Biophysical Journal*. https://doi.org/10.1016/S0006-3495(98)77751-3

Korver, A. M. H., Smith, R. J. H., Van Camp, G., Schleiss, M. R., Bitner-Glindzicz, M. A. K., Lustig, L. R., Usami, S. I., & Boudewyns, A. N. (2017). Congenital hearing loss. *Nature Reviews Disease Primers*. https://doi.org/10.1038/nrdp.2016.94

Krey, J. F., Chatterjee, P., Dumont, R. A., O'Sullivan, M., Choi, D., Bird, J. E., & Barr-Gillespie, P. G. (2020). Mechanotransduction-Dependent Control of Stereocilia Dimensions and Row Identity in Inner Hair Cells. *Current Biology*. https://doi.org/10.1016/j.cub.2019.11.076

Krey, J. F., Krystofiak, E. S., Dumont, R. A., Vijayakumar, S., Choi, D., Rivero, F., Kachar, B., Jones, S. M., & Barr-Gillespie, P. G. (2016). Plastin 1 widens stereocilia by transforming actin filament packing from hexagonal to liquid. *Journal of Cell Biology*. https://doi.org/10.1083/jcb.201606036

Liu, P., Li, H., Ren, X., Mao, H., Zhu, Q., Zhu, Z., Yang, R., Yuan, W., Liu, J., Wang, Q., & Liu, M. (2008). Novel ACTG1 mutation causing autosomal dominant non-syndromic hearing impairment in a Chinese family. *Journal of Genetics and Genomics*. https://doi.org/10.1016/S1673-8527(08)60075-2

Manor, U., Disanza, A., Grati, M., Andrade, L., Lin, H., Di Fiore, P. P., Scita, G., & Kachar, B. (2011). Regulation of stereocilia length by myosin XVa and whirlin depends on the actin-regulatory protein Eps8. *Current Biology*. https://doi.org/10.1016/j.cub.2010.12.046

Mburu, P., Romero, M. R., Hilton, H., Parker, A., Townsend, S., Kikkawa, Y., & Brown, S. D. M. (2010). Gelsolin plays a role in the actin polymerization complex of hair cell stereocilia. *PLoS ONE*. https://doi.org/10.1371/journal.pone.0011627

McGough, A., Pope, B., Chiu, W., & Weeds, A. (1997). Cofilin changes the twist of F-actin: Implications for actin filament dynamics and cellular function. *Journal of Cell Biology*. https://doi.org/10.1083/jcb.138.4.771

Morín, M., Bryan, K. E., Mayo-Merino, F., Goodyear, R., Mencía, Á., Modamio-Høybjør, S., Del Castillo, I., Cabalka, J. M., Richardson, G., Moreno, F., Rubenstein, P. A., & Moreno-Pelayo, M. Á. (2009). In vivo and in vitro effects of two novel gamma-actin (ACTG1) mutations that cause DFNA20/26 hearing impairment. *Human Molecular*

Genetics. https://doi.org/10.1093/hmg/ddp249

NIH. (2019). *Noise-Induced Hearing Loss (NIHL) | NIDCD*. https://www.nidcd.nih.gov/health/noise-induced-hearing-loss

Ó Maoiléidigh, D., & Ricci, A. J. (2019). A Bundle of Mechanisms: Inner-Ear Hair-Cell Mechanotransduction. In *Trends in Neurosciences*. https://doi.org/10.1016/j.tins.2018.12.006

Oesterle, E. C. (2013). Changes in the adult vertebrate auditory sensory epithelium after trauma. In *Hearing Research*. https://doi.org/10.1016/j.heares.2012.11.010

Orr, A. W., Helmke, B. P., Blackman, B. R., & Schwartz, M. A. (2006). Mechanisms of mechanotransduction. In *Developmental Cell*. https://doi.org/10.1016/j.devcel.2005.12.006

Pacentine, I., Chatterjee, P., & Barr-Gillespie, P. G. (2020). Stereocilia rootlets: Actin-based structures that are essential for structural stability of the hair bundle. In *International Journal of Molecular Sciences*. https://doi.org/10.3390/ijms21010324

Pan, B., Akyuz, N., Liu, X. P., Asai, Y., Nist-Lund, C., Kurima, K., Derfler, B. H., György, B., Limapichat, W., Walujkar, S., Wimalasena, L. N., Sotomayor, M., Corey, D. P., & Holt, J. R. (2018). TMC1 Forms the Pore of Mechanosensory Transduction Channels in Vertebrate Inner Ear Hair Cells. *Neuron*. https://doi.org/10.1016/j.neuron.2018.07.033

Patrinostro, X., Roy, P., Lindsay, A., Chamberlain, C. M., Sundby, L. J., Starker, C. G., Voytas, D. F., Ervasti, J. M., & Perrin, B. J. (2018). Essential nucleotide- and protein-dependent functions of Actb/β-actin. *Proceedings of the National Academy of Sciences of the United States of America*. https://doi.org/10.1073/pnas.1807895115

Pepermans, E., & Petit, C. (2015). The tip-link molecular complex of the auditory mechano-electrical transduction machinery. In *Hearing Research*. https://doi.org/10.1016/j.heares.2015.05.005

Perrin, B. J., & Ervasti, J. M. (2010). The actin gene family: Function follows isoform. *Cytoskeleton*. https://doi.org/10.1002/cm.20475

Perrin, B. J., Sonnemann, K. J., & Ervasti, J. M. (2010). β-Actin and γ-Actin are each dispensable for auditory hair cell development but required for stereocilia maintenance. *PLoS Genetics*. https://doi.org/10.1371/journal.pgen.1001158

Pickles, J. O., Comis, S. D., & Osborne, M. P. (1984). Cross-links between stereocilia in the guinea pig organ of Corti, and their possible relation to sensory transduction. *Hearing Research*. https://doi.org/10.1016/0378-5955(84)90041-8

Probst, F. J., Fridell, R. A., Raphael, Y., Saunders, T. L., Wang, A., Liang, Y., Morell, R. J., Touchman, J. W., Lyons, R. H., Noben-Trauth, K., Friedman, T. B., & Camper, S. A. (1998). Correction of deafness in shaker-2 mice by an unconventional myosin in a BAC

transgene. *Science*. https://doi.org/10.1126/science.280.5368.1444

Procaccio, V., Salazar, G., Ono, S., Styers, M. L., Gearing, M., Davila, A., Jimenez, R., Juncos, J., Gutekunst, C. A., Meroni, G., Fontanella, B., Sontag, E., Sontag, J. M., Faundez, V., & Wainer, B. H. (2006). A mutation of β-actin that alters depolymerization dynamics is associated with autosomal dominant developmental malformations, deafness, and dystonia. *American Journal of Human Genetics*. https://doi.org/10.1086/504271

Qing, Z., & Mao-li, D. (2009). Anatomy and physiology of peripheral auditory system and commen causes of hearing loss. In *Journal of Otology*. https://doi.org/10.1016/S1672-2930(09)50002-5

Raphael, Y., & Altschuler, R. A. (2003). Structure and innervation of the cochlea. In *Brain Research Bulletin*. https://doi.org/10.1016/S0361-9230(03)00047-9

Raphael, Y., Kim, Y. H., Osumi, Y., & Izumikawa, M. (2007). Non-sensory cells in the deafened organ of Corti: Approaches for repair. In *International Journal of Developmental Biology*. https://doi.org/10.1387/ijdb.072370yr

Rendtorff, N. D. N. D., Zhu, M., Fagerheim, T., Antal, T. L., Jones, M. P., Teslovich, T. M., Gillanders, E. M., Barmada, M., Teig, E., Trent, J. M., Friderici, K. H., Stephan, D. A., & Tranebjærg, L. (2006). A novel missense mutation in ACTG1 causes dominant deafness in a Norwegian DFNA20/26 family, but ACTG1 mutations are not frequent among families with hereditary hearing impairment. *European Journal of Human Genetics*. https://doi.org/10.1038/sj.ejhg.5201670

Riga, M., Korres, G., Chouridis, P., Naxakis, S., & Danielides, V. (2018). Congenital cytomegalovirus infection inducing non-congenital sensorineural hearing loss during childhood; a systematic review. In *International Journal of Pediatric Otorhinolaryngology*. https://doi.org/10.1016/j.ijporl.2018.10.005

Rivière, J. B., Van Bon, B. W. M., Hoischen, A., Kholmanskikh, S. S., O'Roak, B. J., Gilissen, C., Gijsen, S., Sullivan, C. T., Christian, S. L., Abdul-Rahman, O. A., Atkin, J. F., Chassaing, N., Drouin-Garraud, V., Fry, A. E., Fryns, J. P., Gripp, K. W., Kempers, M., Kleefstra, T., Mancini, G. M. S., … Dobyns, W. B. (2012). De novo mutations in the actin genes ACTB and ACTG1 cause Baraitser-Winter syndrome. *Nature Genetics*. https://doi.org/10.1038/ng.1091

Robles, L., & Ruggero, M. A. (2001). Mechanics of the mammalian cochlea. In *Physiological Reviews*. https://doi.org/10.1152/physrev.2001.81.3.1305

Roizen, N. J. (2003). Nongenetic causes of hearing loss. In *Mental Retardation and Developmental Disabilities Research Reviews*. https://doi.org/10.1002/mrdd.10068

Roth, B., & Bruns, V. (1992). Postnatal development of the rat organ of Corti. *Anatomy and Embryology*. https://doi.org/10.1007/bf00185616

Salt, A. N., & Hirose, K. (2018). Communication pathways to and from the inner ear and their contributions to drug delivery. In *Hearing Research*. https://doi.org/10.1016/j.heares.2017.12.010

Sekerková, G., Richter, C. P., & Bartles, J. R. (2011). Roles of the espin actin-bundling proteins in the morphogenesis and stabilization of hair cell stereocilia revealed in CBA/CaJ congenic jerker mice. *PLoS Genetics*. https://doi.org/10.1371/journal.pgen.1002032

Somlyo, A. P., & Somlyo, A. V. (2003). Ca2+ sensitivity of smooth muscle and nonmuscle myosin II: Modulated by G proteins, kinases, and myosin phosphatase. In *Physiological Reviews*. https://doi.org/10.1152/physrev.00023.2003

Suresh, R., & Diaz, R. J. (2021). The remodelling of actin composition as a hallmark of cancer. In *Translational Oncology*. https://doi.org/10.1016/j.tranon.2021.101051

Tang, J., Taylor, D. W., & Taylor, K. A. (2001). The three-dimensional structure of α-actinin obtained by cryoelectron microscopy suggests a model for Ca2+-dependent actin binding. *Journal of Molecular Biology*. https://doi.org/10.1006/jmbi.2001.4789

Tilney, L. G., Derosier, D. J., & Mulroy, M. J. (1980). The organization of actin filaments in the stereocilia of cochlear hair cells. *Journal of Cell Biology*. https://doi.org/10.1083/jcb.86.1.244

Van Wijk, E., Krieger, E., Kemperman, M. H., De Leenheer, E. M. R., Huygen, P. L. M., Cremers, C. W. R. J., Cremers, F. P. M., & Kremer, H. (2003). A mutation in the gamma actin 1 (ACTG1) gene causes autosomal dominant hearing loss (DFNA20/26). *Journal of Medical Genetics*. https://doi.org/10.1136/jmg.40.12.879

Vélez-Ortega, A. C., Freeman, M. J., Indzhykulian, A. A., Grossheim, J. M., & Frolenkov, G. I. (2017). Mechanotransduction current is essential for stability of the transducing stereocilia in mammalian auditory hair cells. *ELife*. https://doi.org/10.7554/eLife.24661

Vélez-Ortega, A. C., & Frolenkov, G. I. (2019). Building and repairing the stereocilia cytoskeleton in mammalian auditory hair cells. In *Hearing Research*. https://doi.org/10.1016/j.heares.2018.12.012

Widmaier, E. P., Raff, H., Strang, K. T., & Vander, A. J. (2019). *Human Physiology: The mechanisms of human function* (15th ed.). Mc Graw Hill Education.

Winkelman, J. D., Suarez, C., Hocky, G. M., Harker, A. J., Morganthaler, A. N., Christensen, J. R., Voth, G. A., Bartles, J. R., & Kovar, D. R. (2016). Fascin- and α-Actinin-Bundled Networks Contain Intrinsic Structural Features that Drive Protein Sorting. *Current Biology*. https://doi.org/10.1016/j.cub.2016.07.080

Zhu, M., Yang, T., Wei, S., DeWan, A. T., Morell, R. J., Elfenbein, J. L., Fisher, R. A., Leal, S. M., Smith, R. J. H., & Friderici, K. H. (2003). Mutations in the γ-Actin Gene (ACTG1) Are Associated with Dominant Progressive Deafness (DFNA20/26). *American Journal*

of Human Genetics. https://doi.org/10.1086/379286

ANNEXES

Annex 1: Animal Protocol 2020-3535 approved for Velez Lab at UK

Annex 2: EIA University Ethical Committee Approval

Annex 3: Mouse Dissection Procedure

Annex 4: Neonatal Cochlea Dissection Procedure